

# Dependency of Gabor Lens Focusing Characteristics on Nonneutral Plasma Properties

Kathrin Schulte

HIC for FAIR Workshop

Riezlern, 14.03.2013



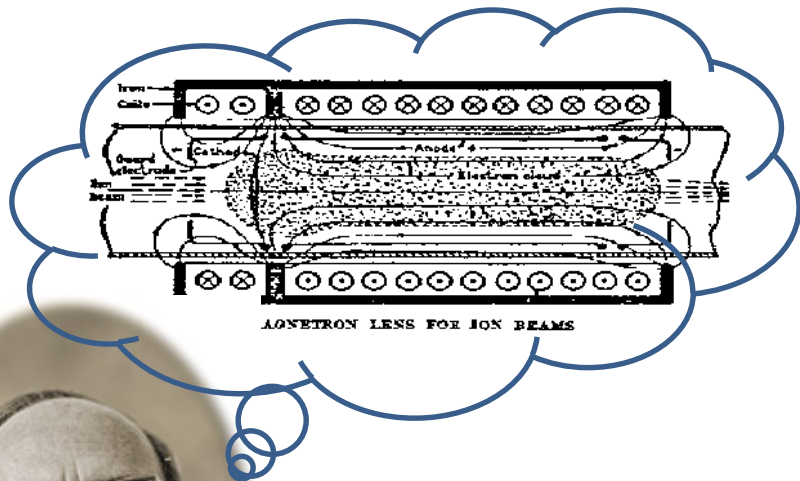
# Outline

1. Motivation and Introduction
2. Diagnostics
3. Beam Transport Measurements and NNP Studies
4. Summary

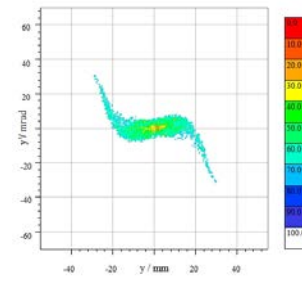
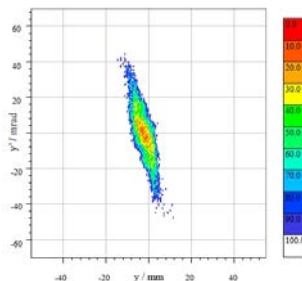
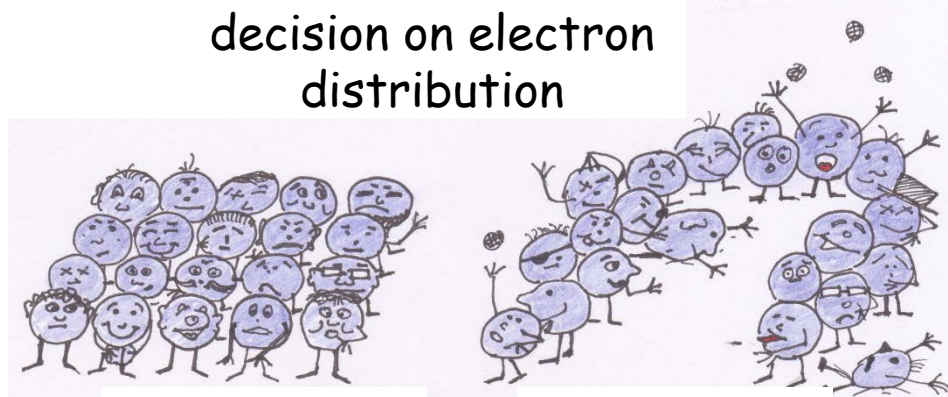
# 1. Motivation and Introduction

# 1.1. Relevant to know about Gabor lenses...

...or Gabor lens in a nutshell



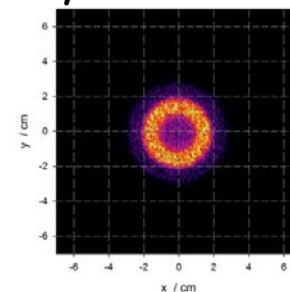
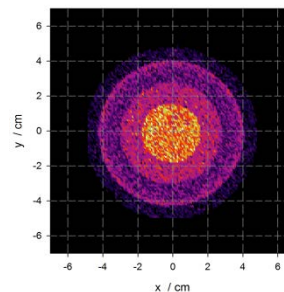
decision on electron distribution



focal length:

$$\frac{1}{f_G} = \frac{qen_e}{2m_i v_i^2 \epsilon_0} l = \frac{en_e}{4\epsilon_0 W_b} l$$

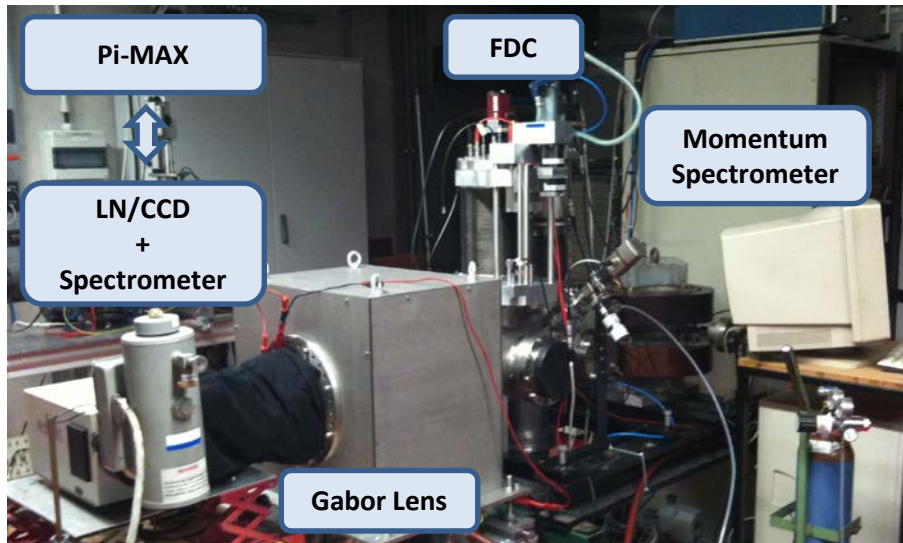
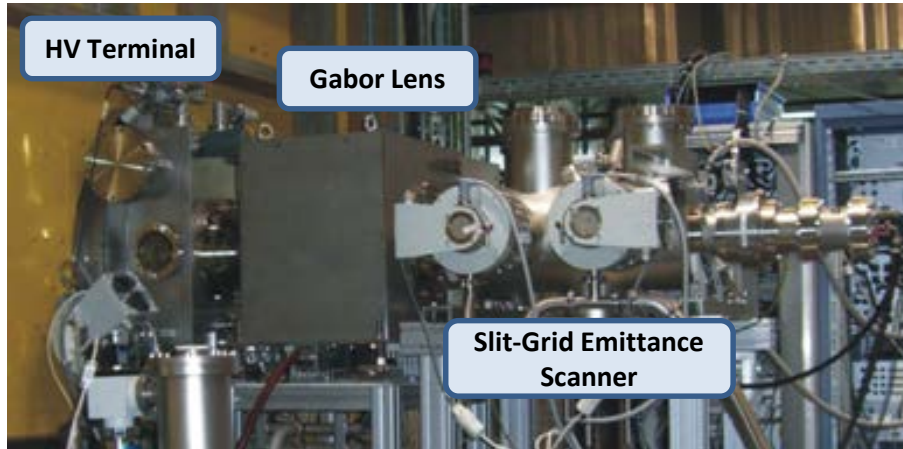
electron cloud dynamics



Dennis Gabor  
 (1900-1979)

*"a beam focusing device that maintains full beam neutralization even for high current beams under all circumstances."*

## 1.2. Investigation of NNP Properties



For the same Gabor lens parameters

### Beam Transport Measurements

-- "with beam"

- Beam Emittance
- Electron Density

and

### Measurements of NNP Properties

-- "without beam"

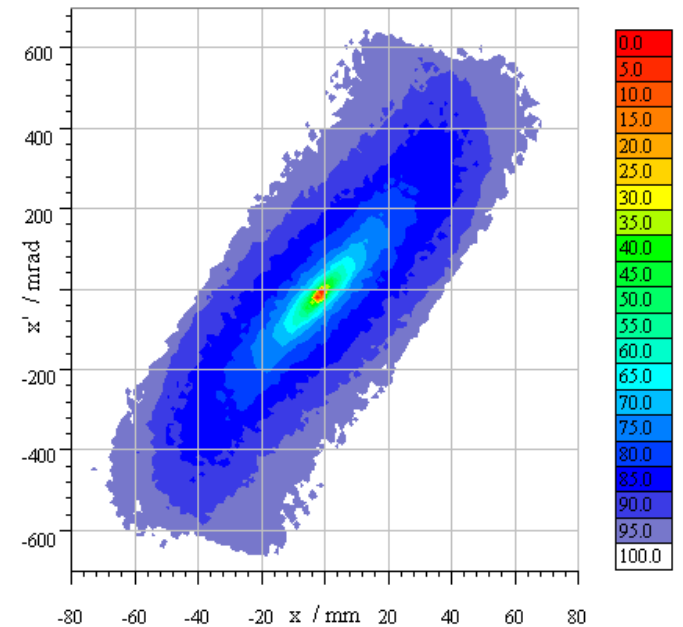
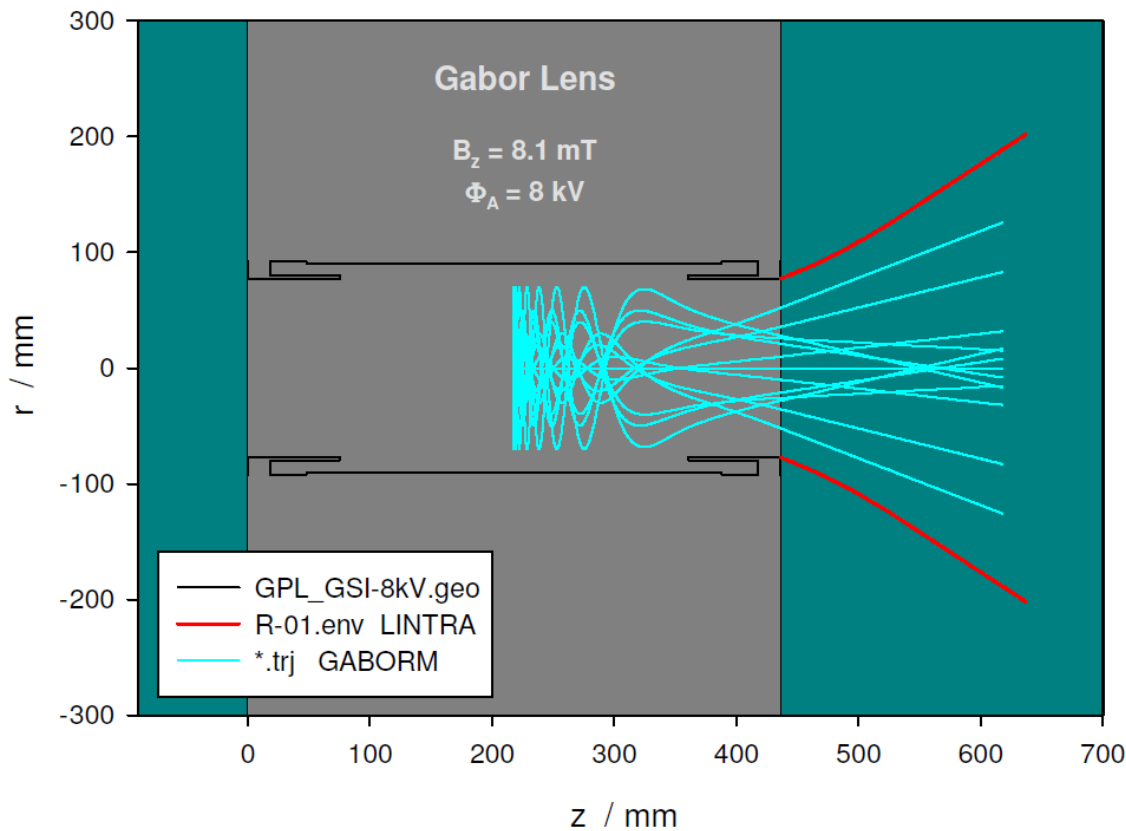
- Electron Density
- Electron Temperatur
- Electron Density Distribution

were performed.

## 2. Diagnostics

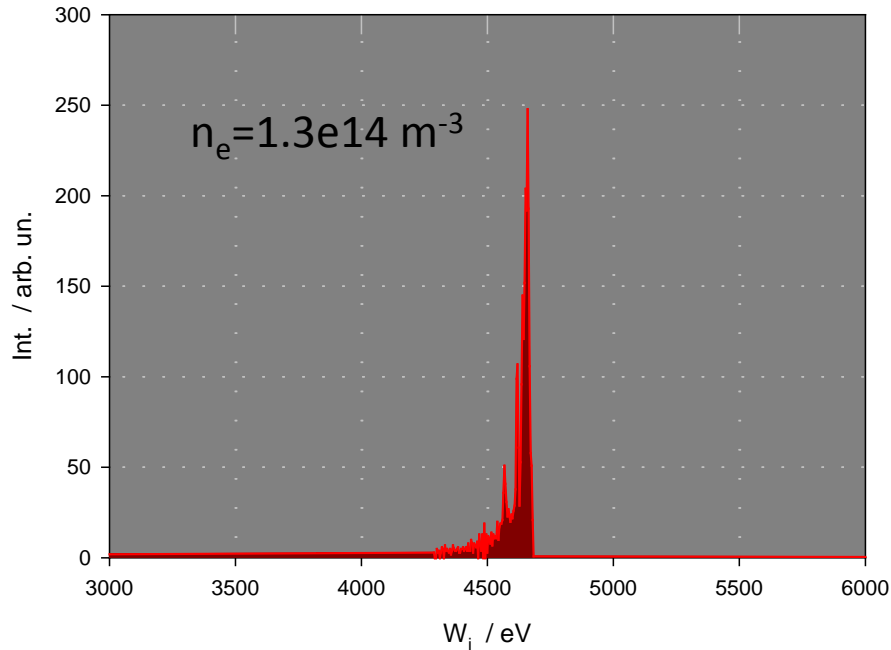
# 2.1. Density Measurement - without beam

simulation of  $\text{Ar}^+$  production assuming a homogeneously distributed residual gas at room temperature 0.025eV (642000 particles)

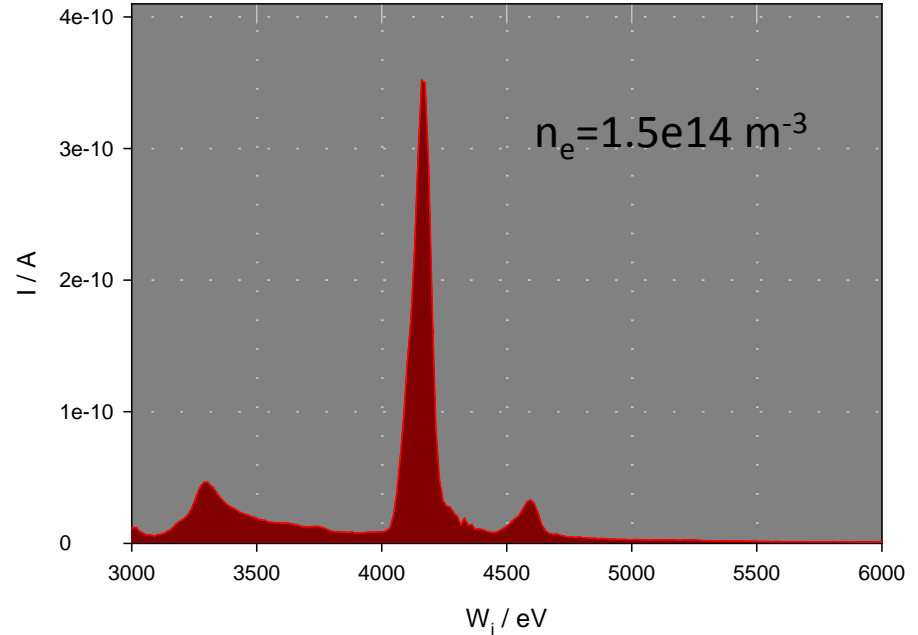


## 2.2. Density Measurement - without beam

simulated energy spectrum



measured energy spectrum



The residual gas ions gain their kinetic energy  $W_i = e\Phi_{\text{ion}}$  within the anode potential  $\Phi_{\text{anode}}$  that is reduced by confined electrons. The electron density is then calculated by

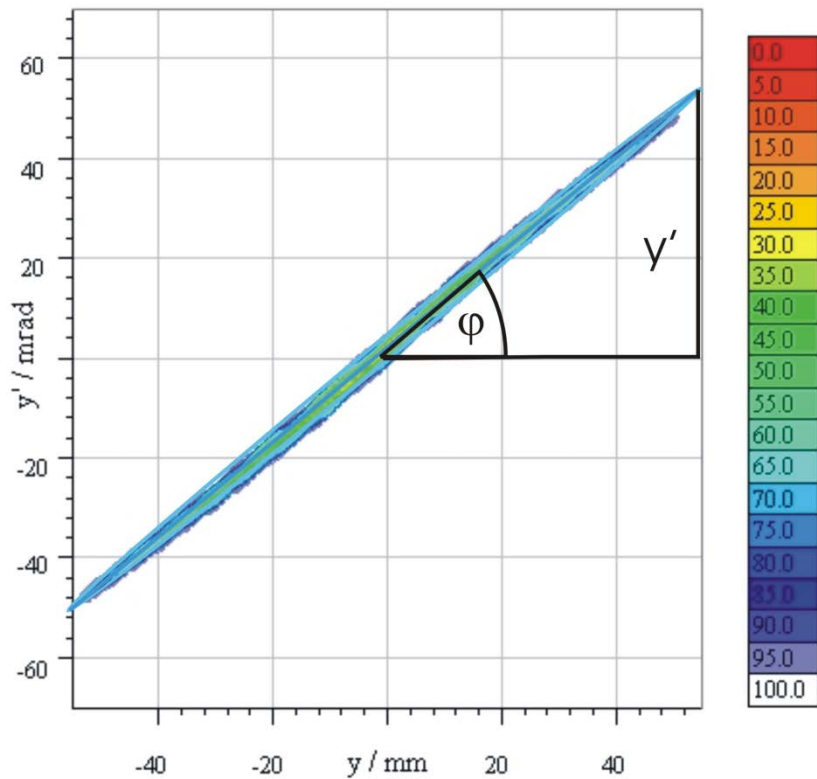
$$n_{e,l} = \frac{4\epsilon_0 \cdot \Delta\Phi}{er^2}$$

assuming  $\Delta\Phi = \Phi_{\text{anode}} - \Phi_{\text{ion}}$



## 2.3. Density Measurement - with beam

change of angle in the phase space distribution → electron density



$$\varphi = \frac{\arctan \frac{2 \cdot \alpha}{\beta \cdot \gamma}}{2}$$

$$y' = \tan(\varphi) \cdot y$$

$$\frac{1}{f} = \frac{\Delta y'}{y} = k_G^2 = \frac{en_e l}{4\epsilon_0 U}$$

$$n_e = \frac{4\epsilon_0 U}{e \cdot l} \frac{\Delta y'}{y}$$

## 2.4. Light Density Distribution and Symmetry

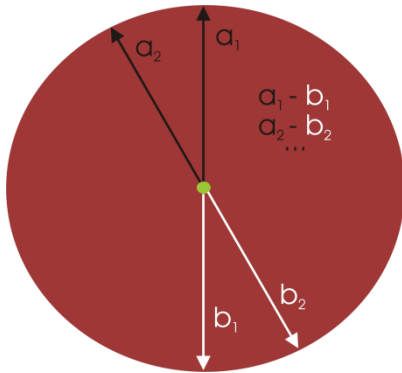
symmetry  $S_{sym}$ :

$$S_{sym} = \frac{\mu_I}{\sigma_I^2}$$

$$\mu_I = \frac{1}{N} \sum_{i=1}^N \int_0^R I(r, \frac{2\pi \cdot i}{N}) dr$$

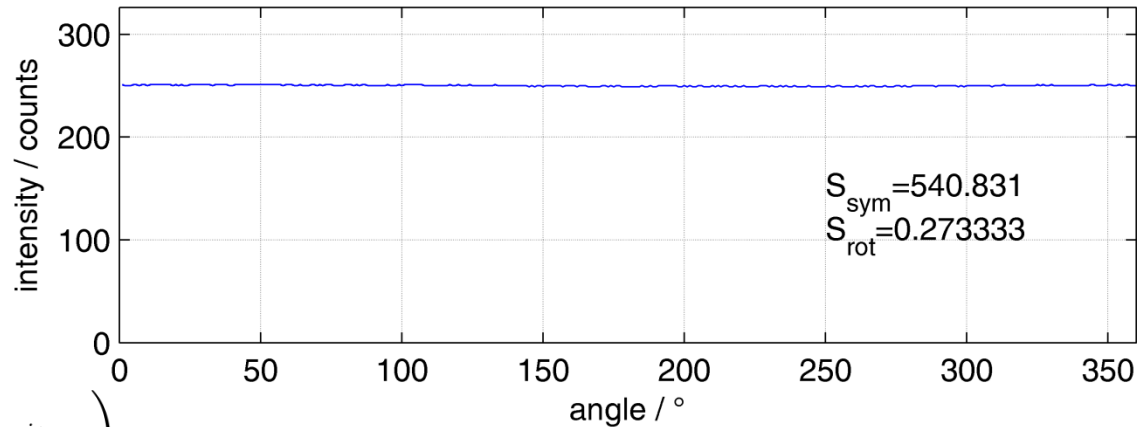
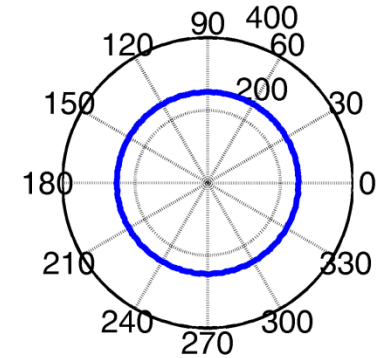
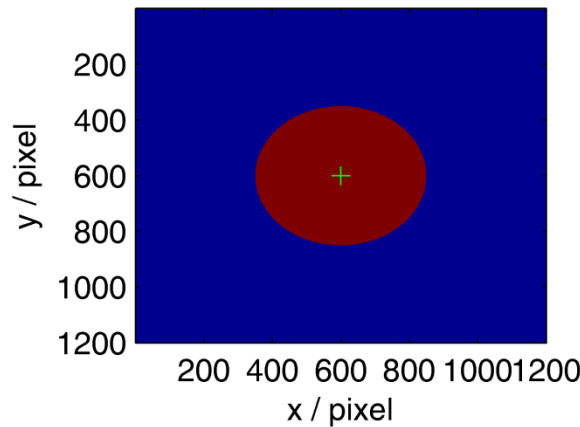
$$\sigma_I^2 = \frac{1}{N} \sum_{i=1}^N \left( \int_0^R I(r, \frac{2\pi \cdot i}{N}) dr - \mu_I \right)^2$$

rotational symmetry  $S_{rot}$ :



$$S_{rot} = \sum_{i=1}^N \left( \sum_{i=1}^{\frac{N}{2}} \int_0^R I(r, \frac{2\pi \cdot i}{N}) dr - \sum_{i=\frac{N}{2}+1}^N \int_0^R I(r, \frac{2\pi \cdot i}{N}) dr \right)$$

evaluation of method for symmetry determination



## 2.4. Light Density Distribution and Symmetry

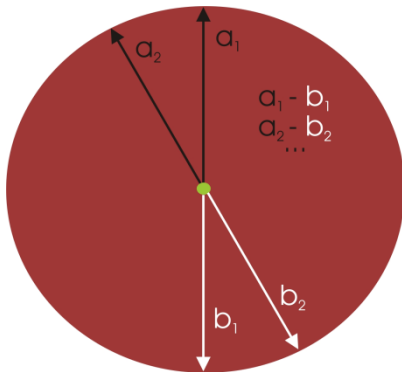
symmetry  $S_{sym}$ :

$$S_{sym} = \frac{\mu_I}{\sigma_I^2}$$

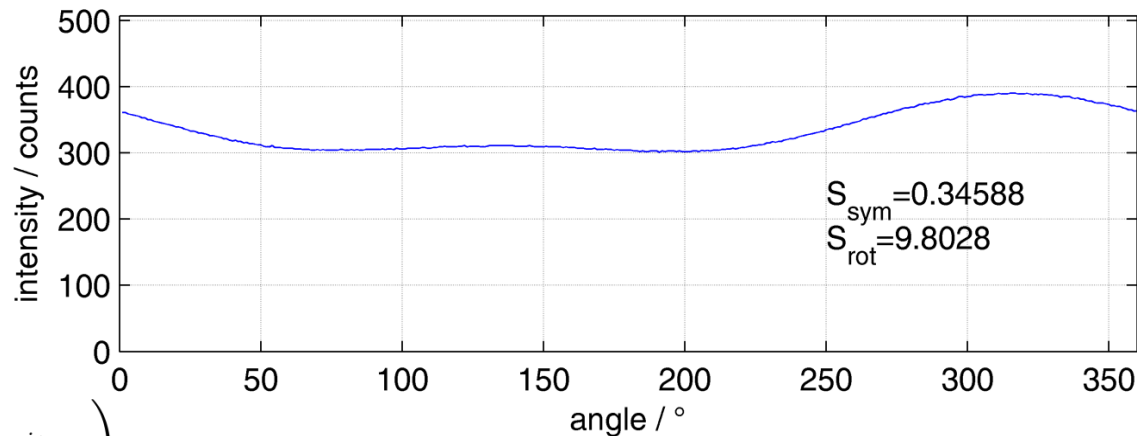
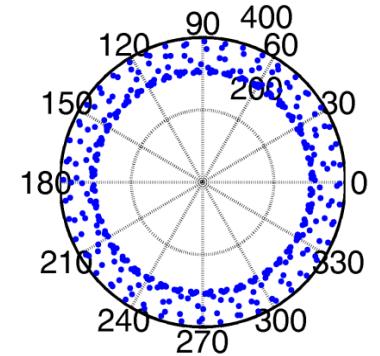
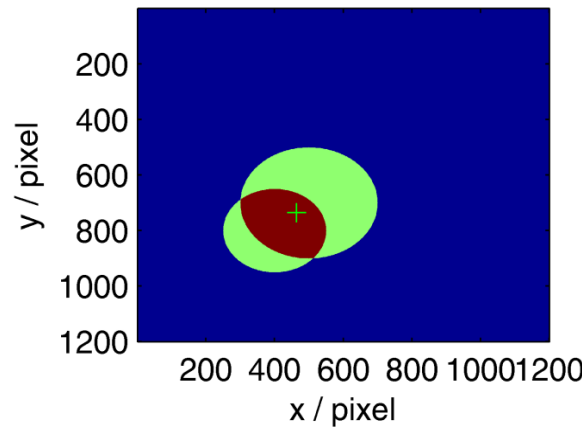
$$\mu_I = \frac{1}{N} \sum_{i=1}^N \int_0^R I(r, \frac{2\pi \cdot i}{N}) dr$$

$$\sigma_I^2 = \frac{1}{N} \sum_{i=1}^N \left( \int_0^R I(r, \frac{2\pi \cdot i}{N}) dr - \mu_I \right)^2$$

rotational symmetry  $S_{rot}$ :



evaluation of method for symmetry determination



$$S_{rot} = \sum_{i=1}^N \left( \sum_{i=1}^{\frac{N}{2}} \int_0^R I(r, \frac{2\pi \cdot i}{N}) dr - \sum_{i=\frac{N}{2}+1}^N \int_0^R I(r, \frac{2\pi \cdot i}{N}) dr \right)$$

## 2.4. Light Density Distribution and Symmetry

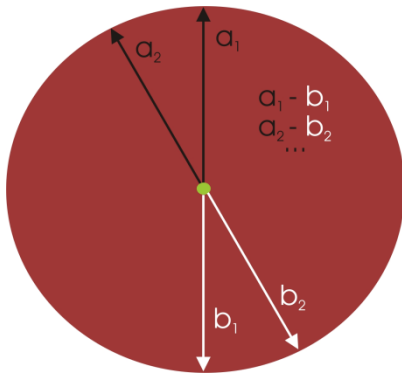
symmetry  $S_{sym}$ :

$$S_{sym} = \frac{\mu_I}{\sigma_I^2}$$

$$\mu_I = \frac{1}{N} \sum_{i=1}^N \int_0^R I(r, \frac{2\pi \cdot i}{N}) dr$$

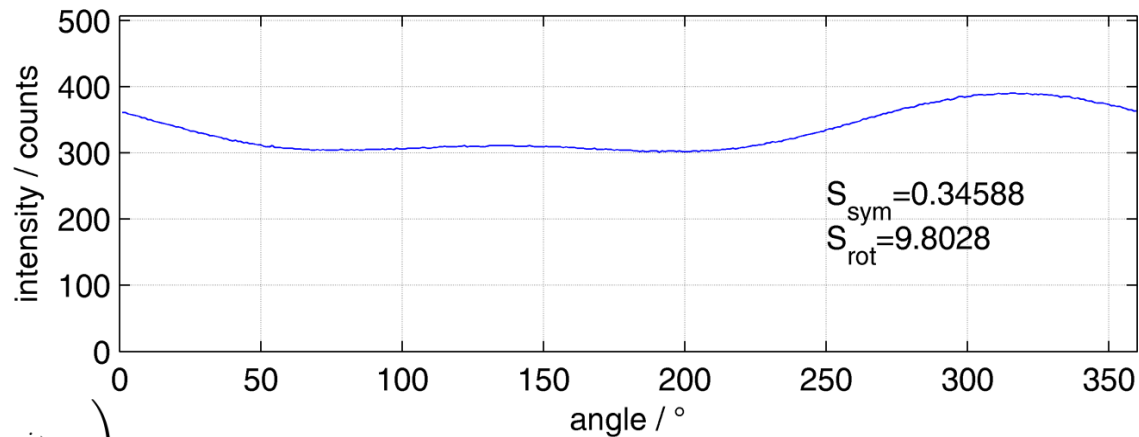
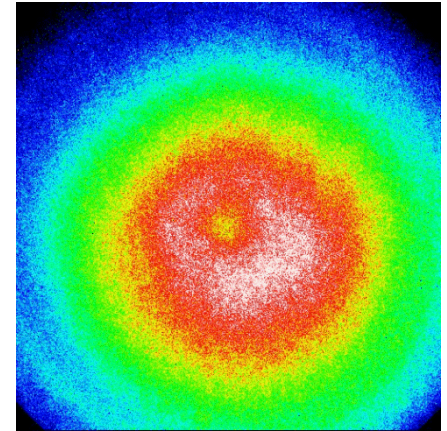
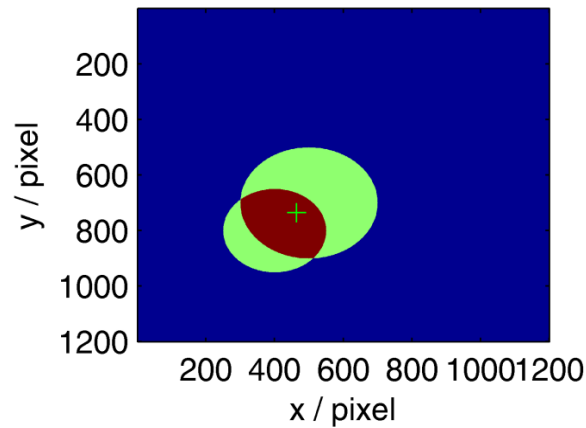
$$\sigma_I^2 = \frac{1}{N} \sum_{i=1}^N \left( \int_0^R I(r, \frac{2\pi \cdot i}{N}) dr - \mu_I \right)^2$$

rotational symmetry  $S_{rot}$ :



$$S_{rot} = \sum_{i=1}^N \left( \sum_{i=1}^{\frac{N}{2}} \int_0^R I(r, \frac{2\pi \cdot i}{N}) dr - \sum_{i=\frac{N}{2}+1}^N \int_0^R I(r, \frac{2\pi \cdot i}{N}) dr \right)$$

evaluation of method for symmetry determination

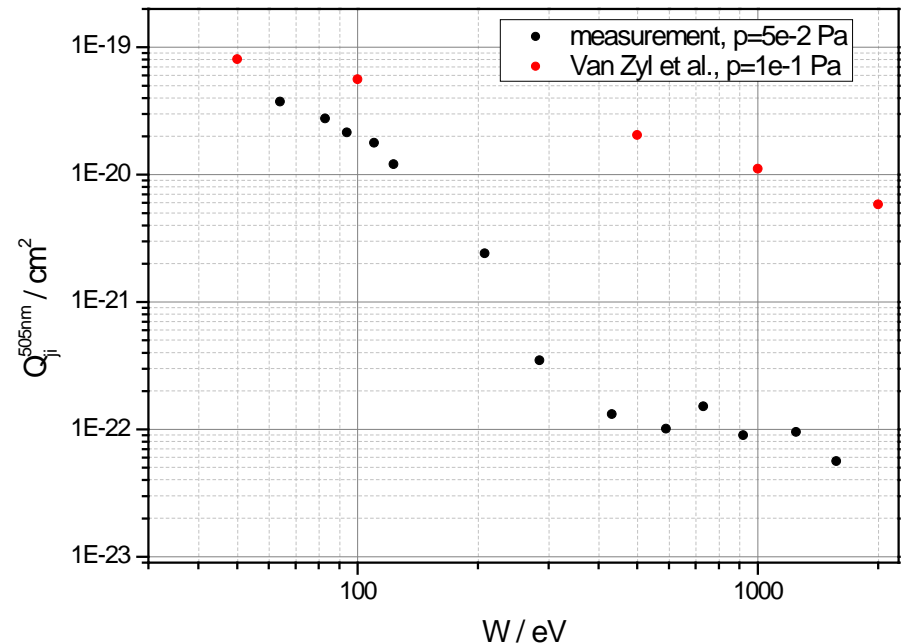
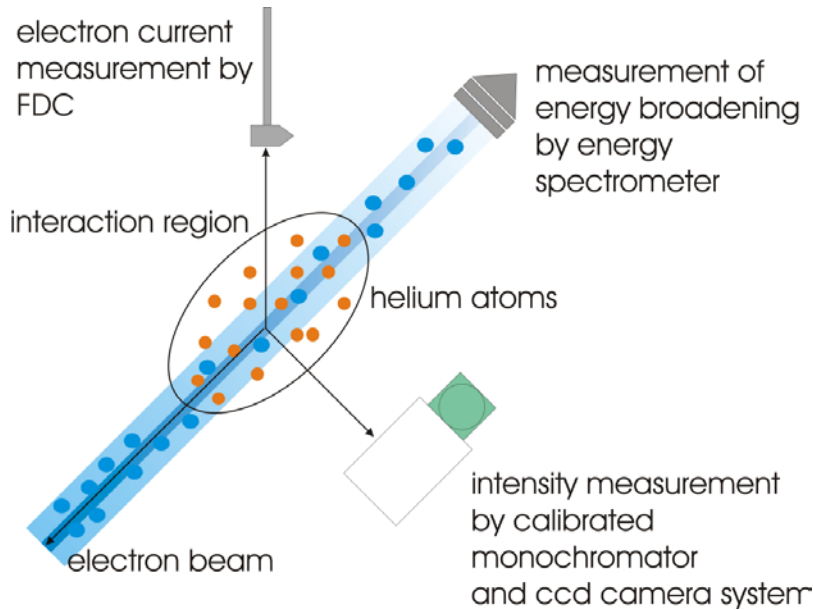


# 2.5. Electron Temperature Measurement

Temperature measurement by optical emission cross sections assuming a corona regime\*:

$$\frac{\Phi_{ij}^{obs}}{\Phi_{ab}^{obs}} = \frac{\int_{E1}^{\infty} Q_{ij}^{opt}(E) \exp[-E/kT_e] E dE}{\int_{E2}^{\infty} Q_{ab}^{opt}(E) \exp[-E/kT_e] E dE} \xrightarrow{\text{simplified}} \frac{\Phi_{ij}^{obs}}{\Phi_{ab}^{obs}} = \frac{Q_{ij}^{opt}(E)}{Q_{ab}^{opt}(E)}$$

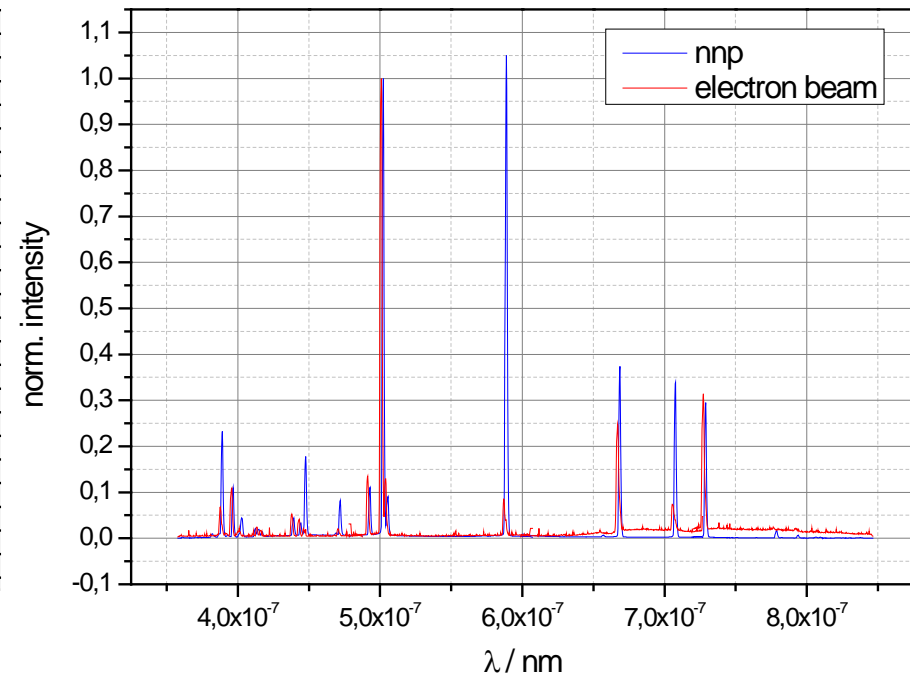
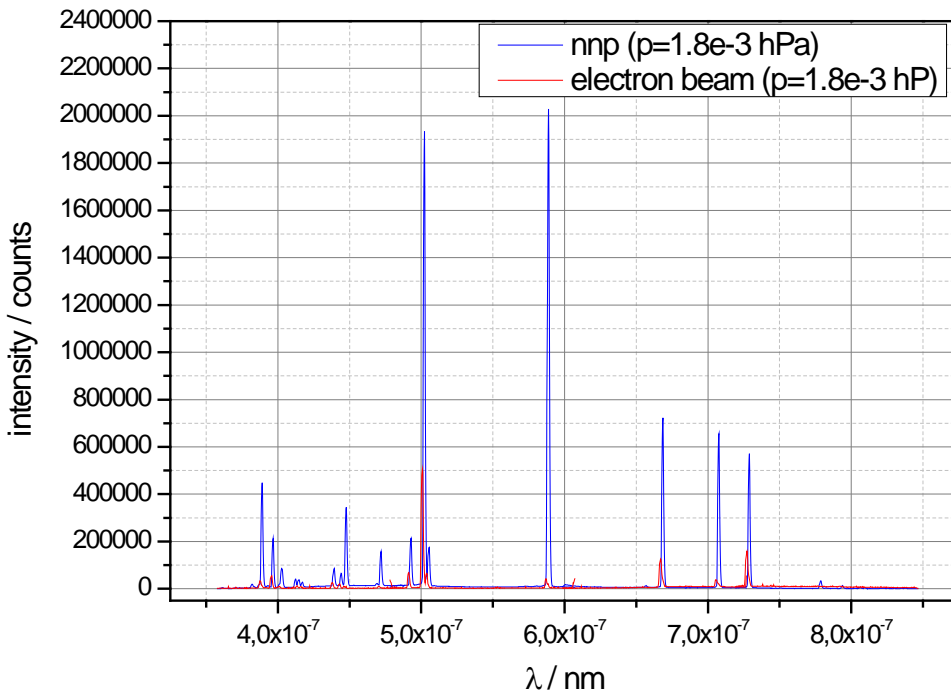
## Measurement of Optical Emission Cross Sections for Helium



\*"Application of excitation cross sections to optical plasma diagnostics", J.B. Boffard, J. Phys. D: Appl. Phys. 37 (2004) R143-R161

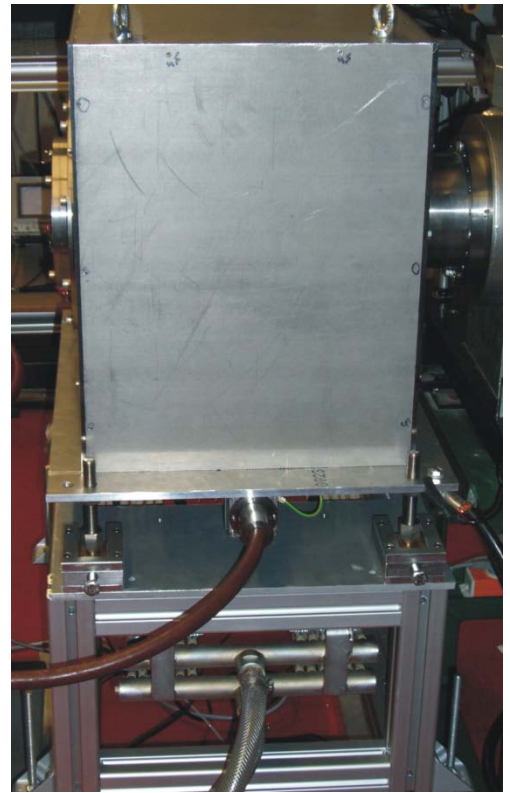
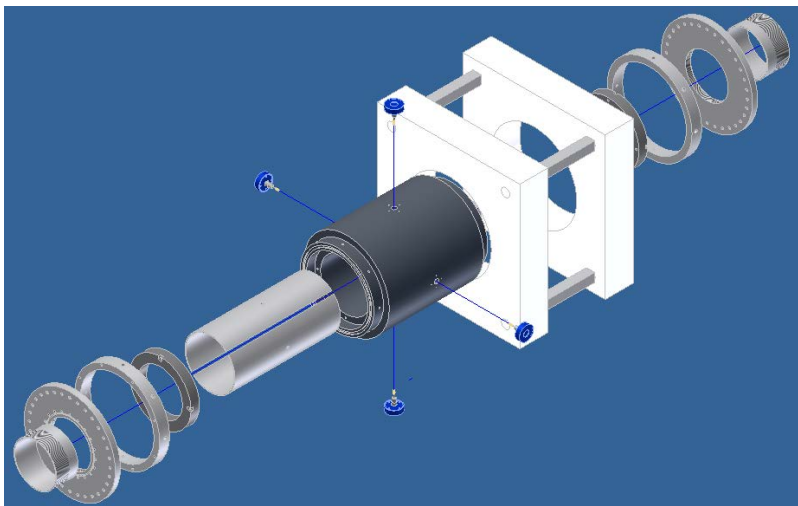
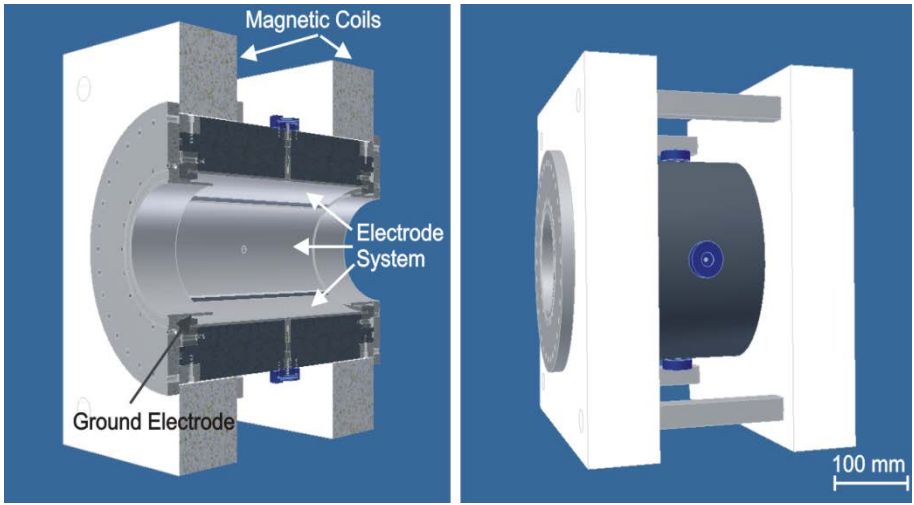
## 2.5. Electron Temperature Measurement

comparison of plasma emission spectra to line emission of atoms excited by an incident electron beam



### 3. Beam Transport Measurements and NNP Studies

# 3.1. Gabor Lens - Specifications



**geometry:**

- $r_{\text{anode}}$ : 85 mm
- $r_{\text{ground}}$ : 75 mm
- $l_{\text{anode}}$ : 340 mm
- $L_{\text{total}}$ : 436 mm

**maximum field and potential**

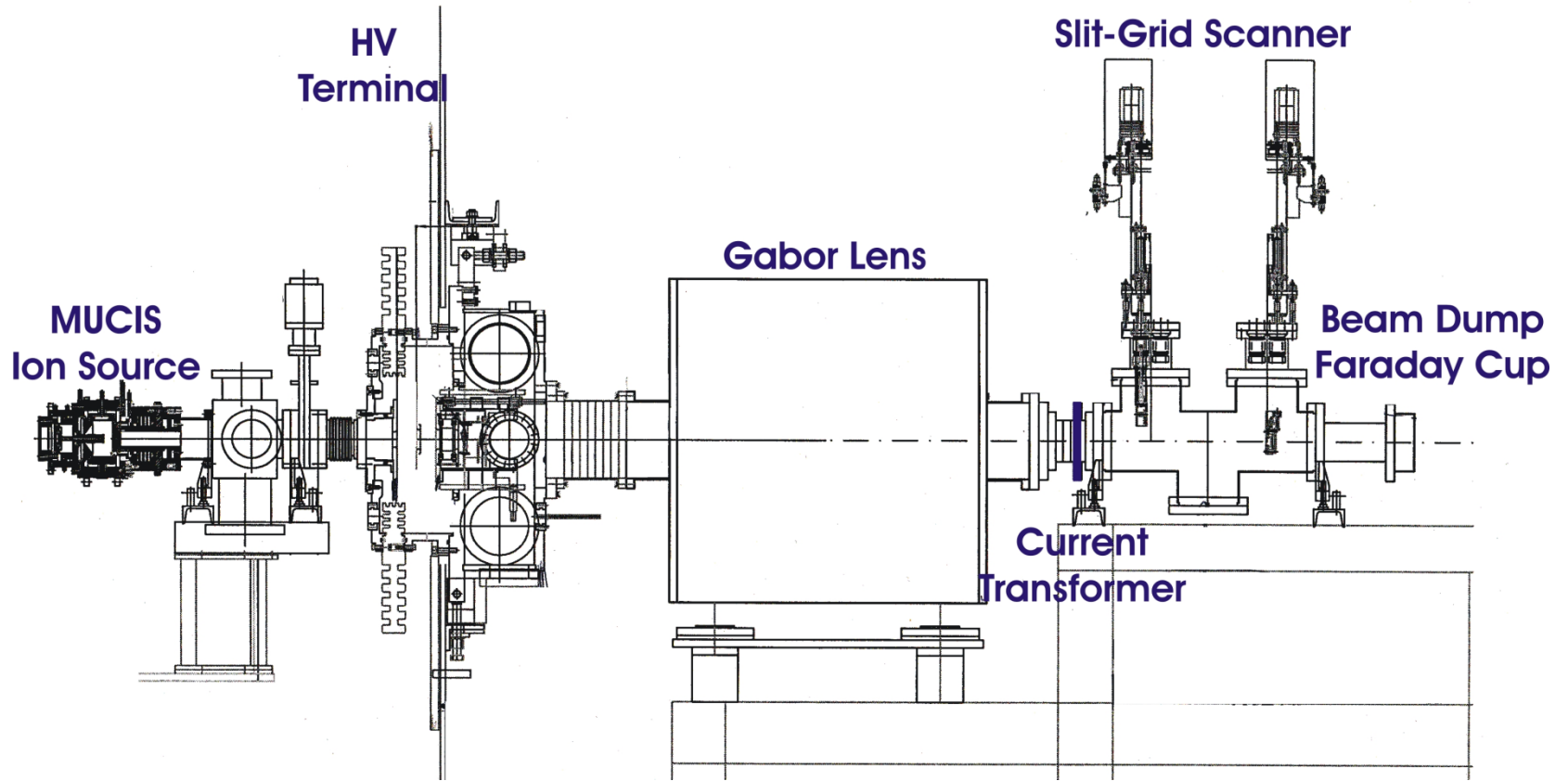
- $B_{z,\text{max}}$ : 160 mT (200 mT)
- $\Phi_{A,\text{max}}$ : 50 kV

**material:**

- stainless steel
- Vinidur ( $T_{\text{max}}=80^{\circ}\text{C}$ ; 14 kV/mm)



## 3.2. High Current Test Injector at GSI



beam parameters: pulse length=1.25 ms, pulse delay=1 Hz

## 3.3. Results

### 1. Low current measurements for studies of the quality of ion optics

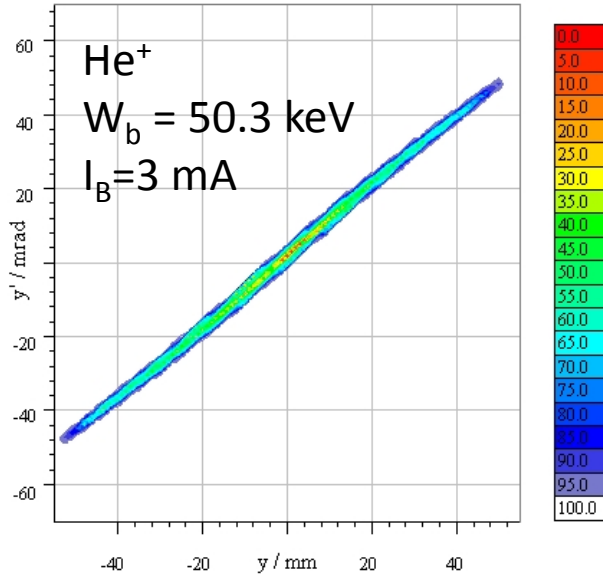
- He<sup>+</sup>,  $W_B=50.3$  keV (12.6 keV/u),  $I_B=3-5$  mA (measured in current transformer behind lens)
- simulated phase space distributions were "fitted" to results of experiments to study the influence of electron density and electron density distribution of the NNP on the ion beam
- NNP studies "without beam" in comparison to the results of beam transport measurements

### 2. High current measurements for studies of the influence on $n_i/n_e$ -ratio

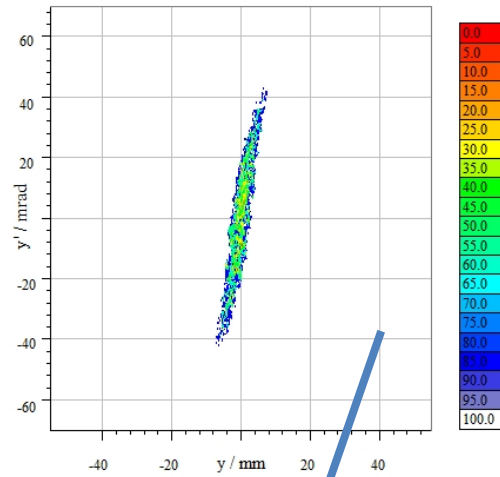
- Installed aperture of 50 mm to save insulator from beam
- Ar<sup>+</sup>,  $W_B=124$  keV (3.1 keV/u),  $I_B=29-35$  mA (measured in current transformer behind lens)
- NNP studies "without beam" in comparison to the results of beam transport measurements

# 3.3. Low Current Measurements

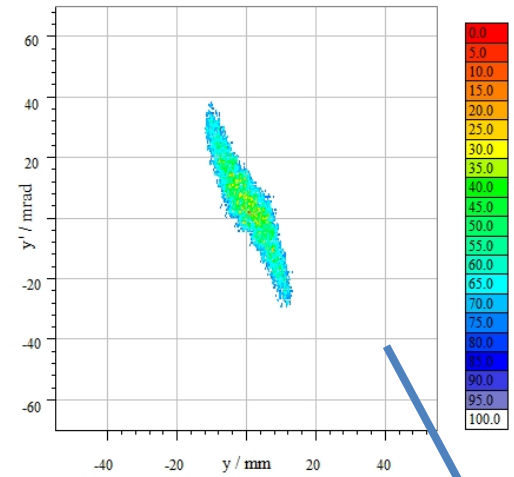
drifted beam



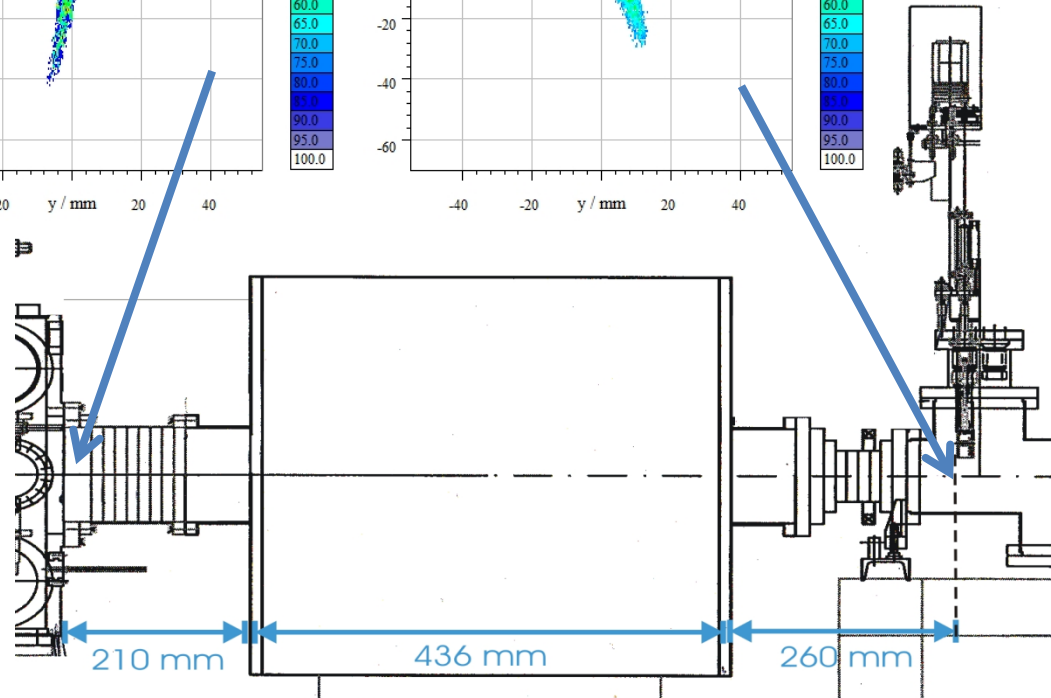
input emittance



transported beam

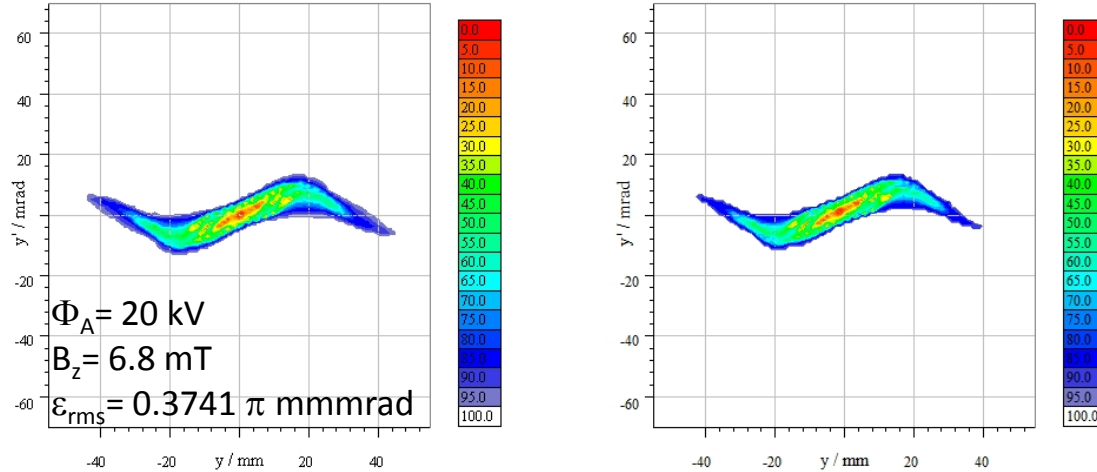


$\Phi_A = 0 \text{ kV}$   
 $B_z = 0 \text{ mT}$   
 $\epsilon_{100\%} = 3568.24 \text{ mm mrad}$   
 $\epsilon_{97\%} = 122.25 \text{ mm mrad}$   
 $\epsilon_{\text{rms}} = 0.16558 \pi \text{ mm mrad}$   
 $\omega = 2.25869$   
 $n = 1$

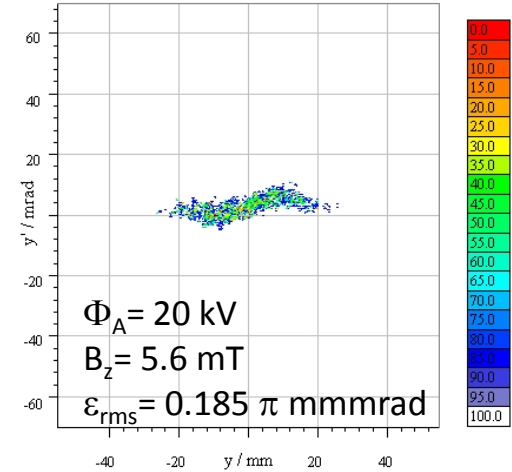


# 3.3. Low Current Measurements

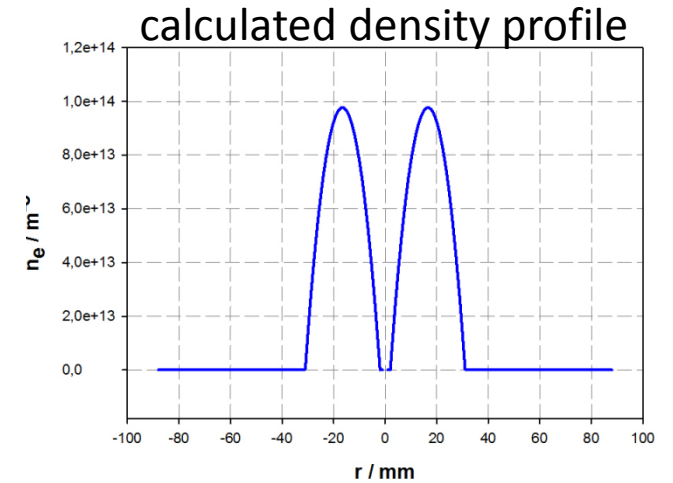
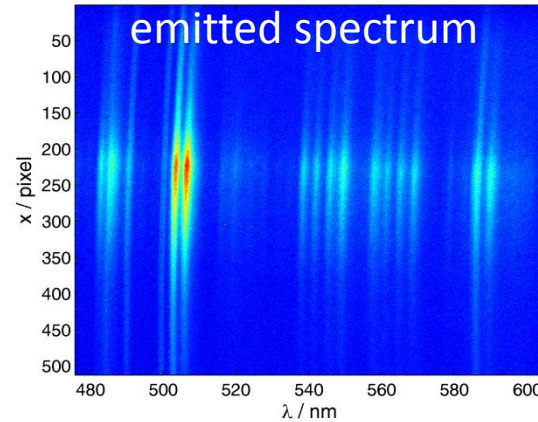
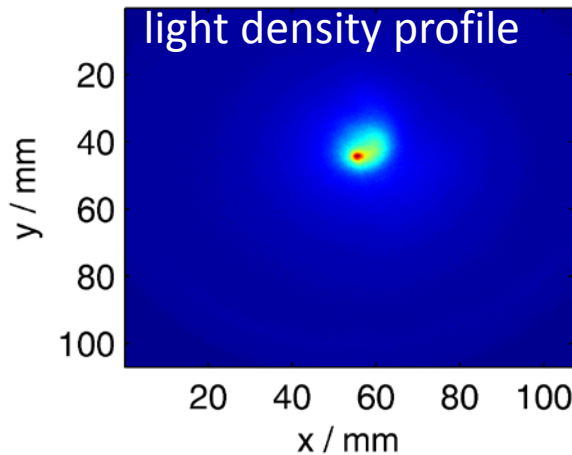
beam transport measurement



numerical simulation

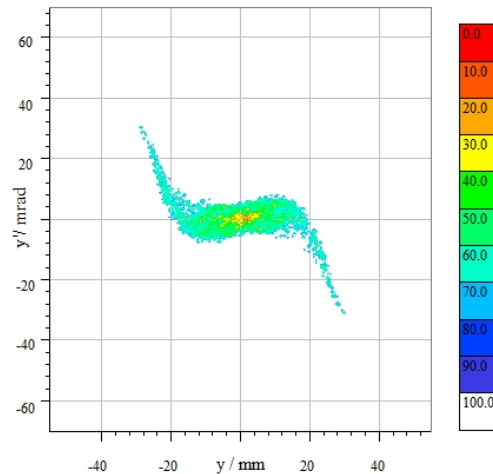
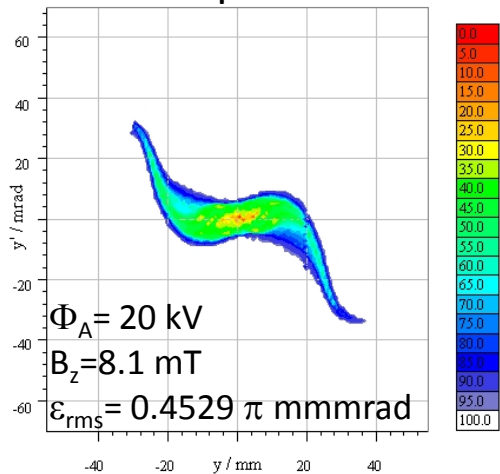


NNP diagnostics

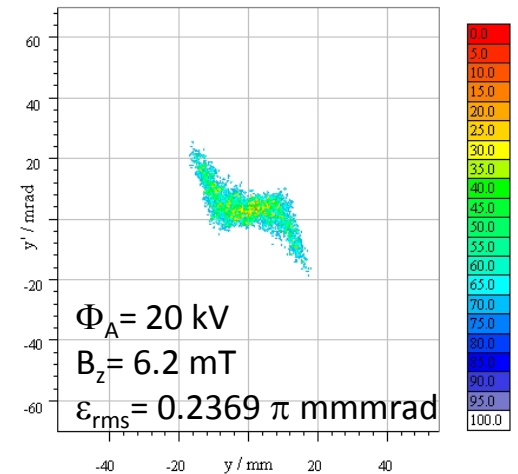


# 3.3. Low Current Measurements

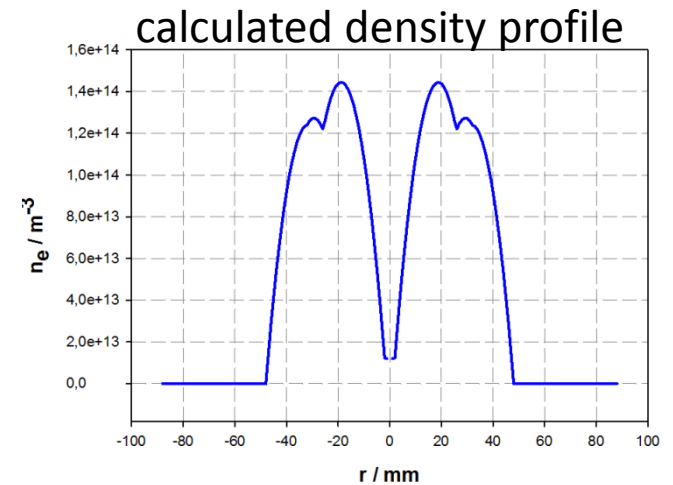
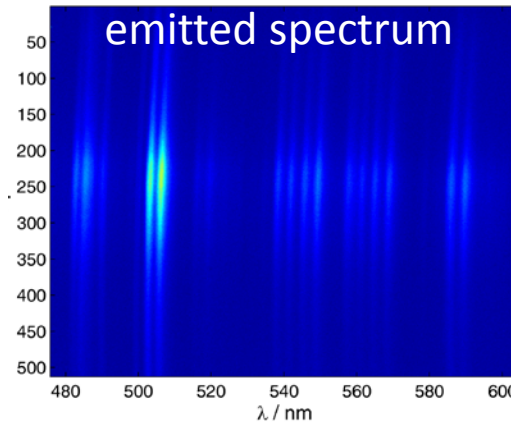
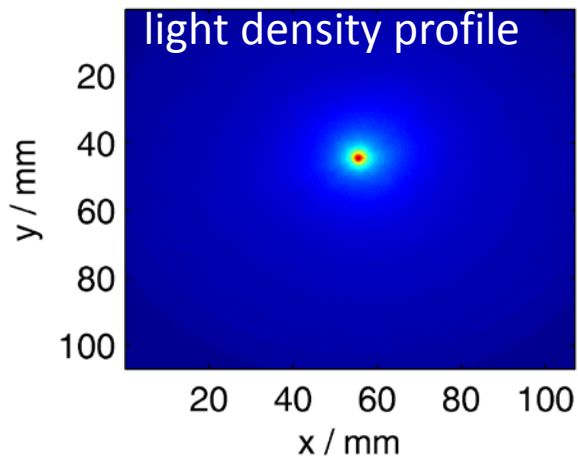
beam transport measurement



numerical simulation

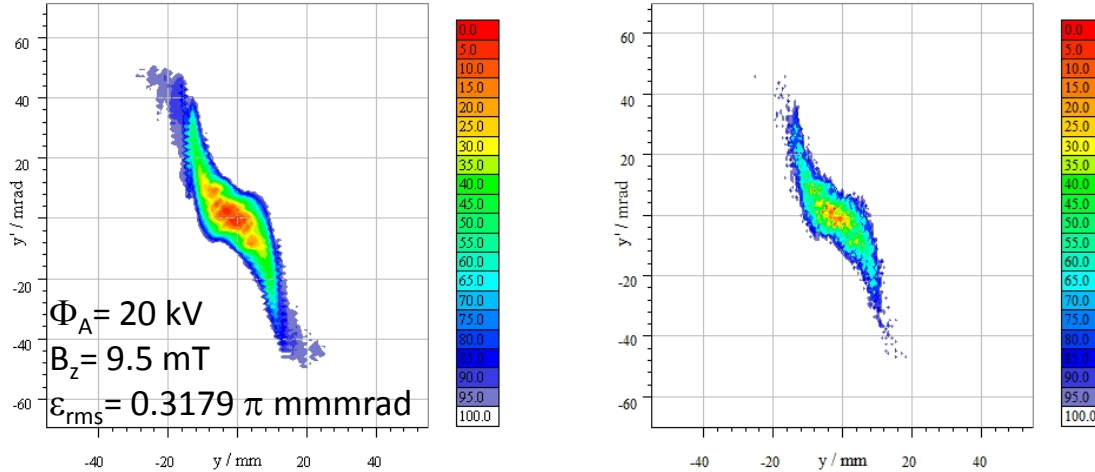


NNP diagnostics

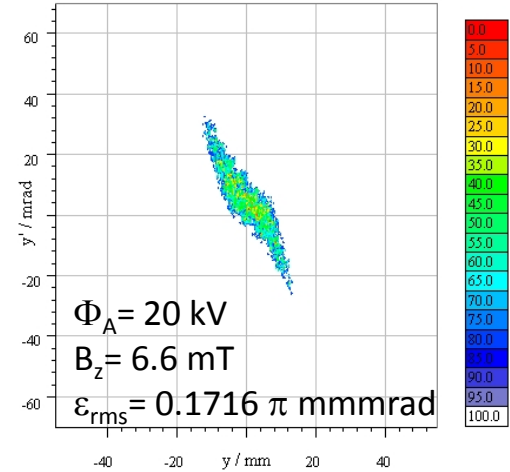


# 3.3. Low Current Measurements

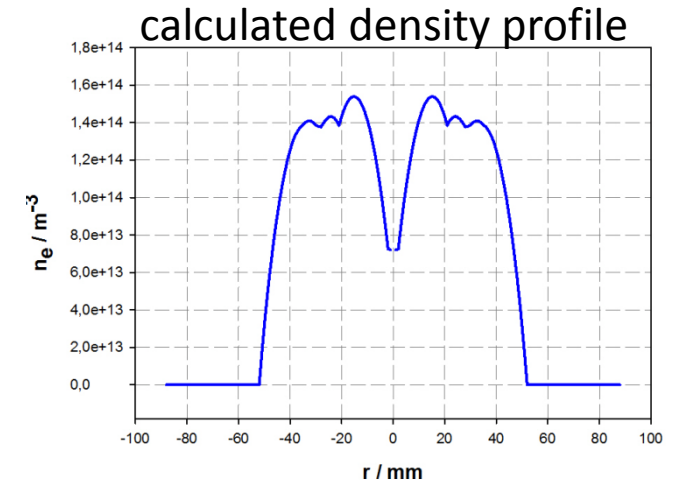
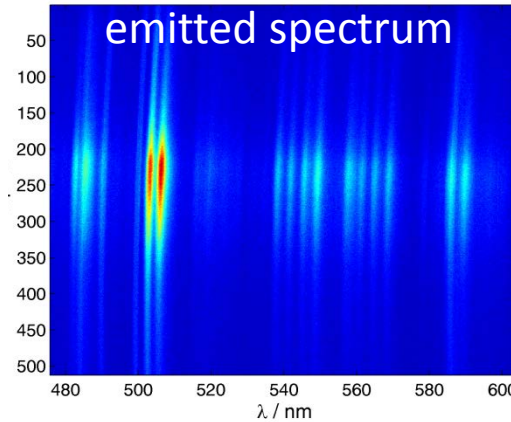
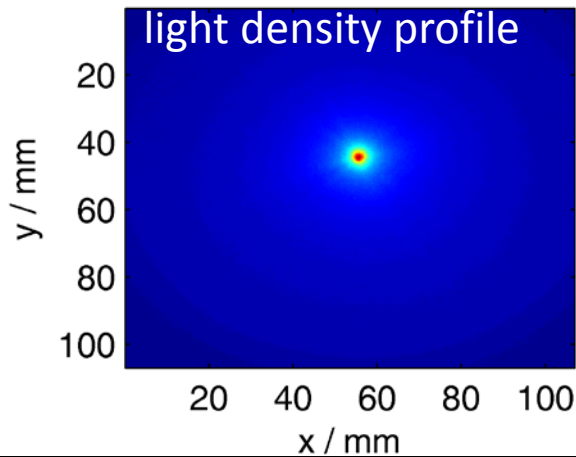
beam transport measurement



numerical simulation

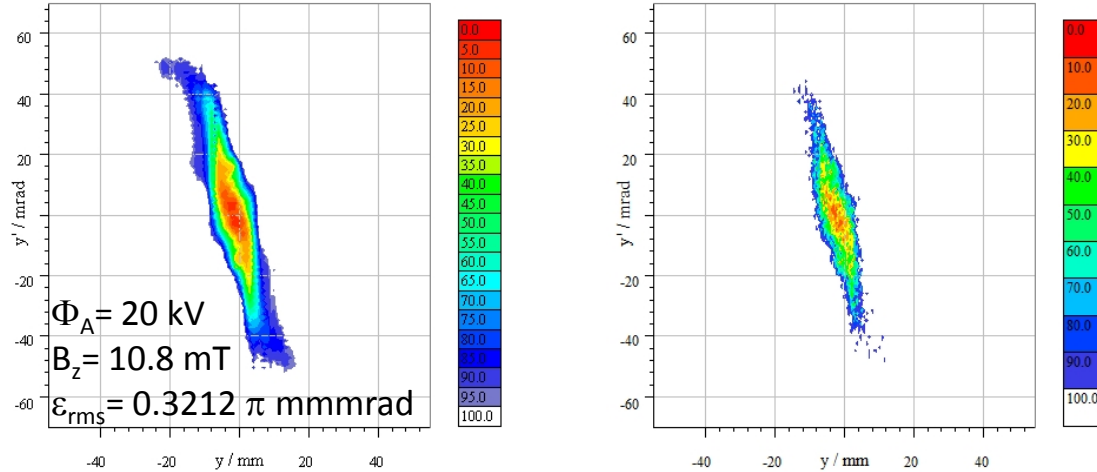


NNP diagnostics

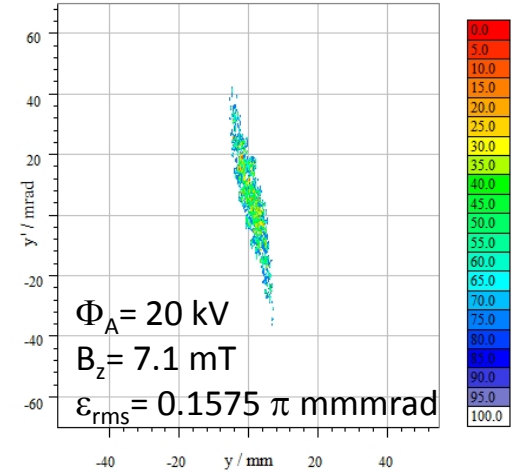


# 3.3. Low Current Measurements

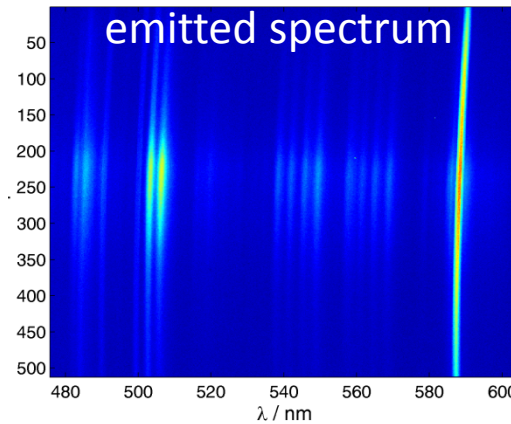
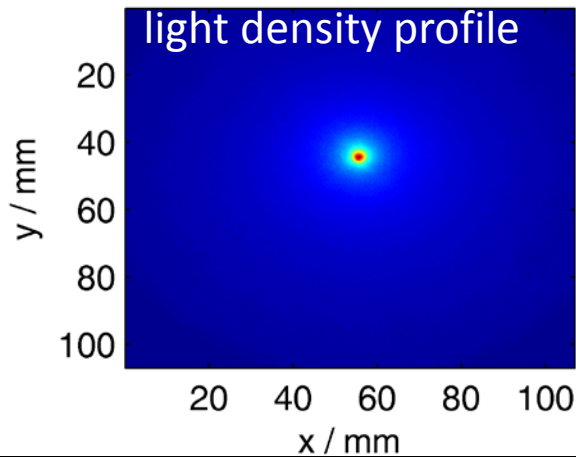
beam transport measurement



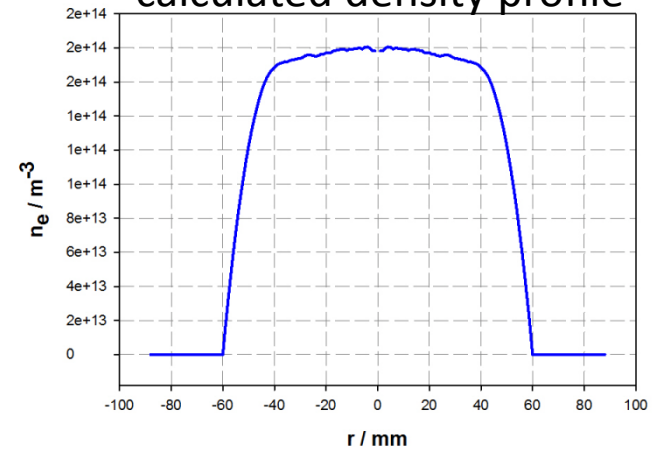
numerical simulation



NNP diagnostics

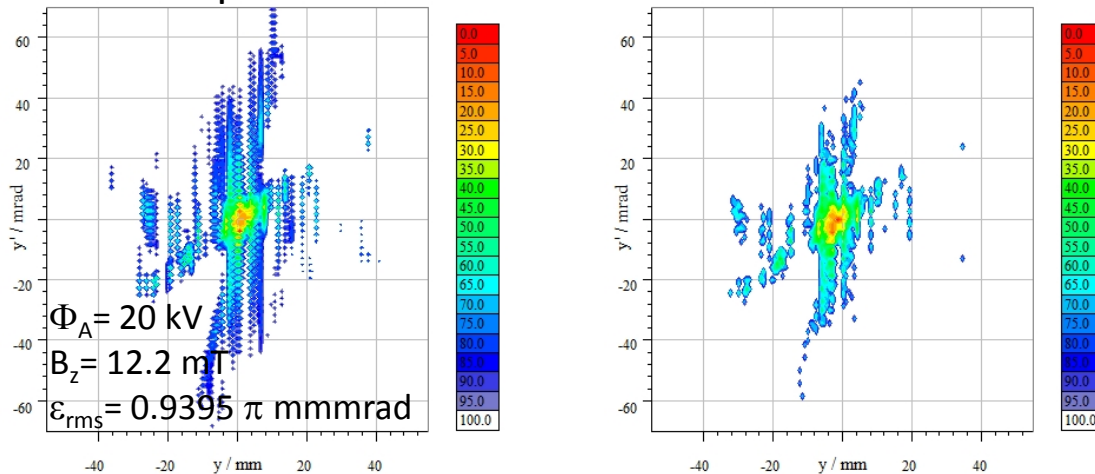


calculated density profile

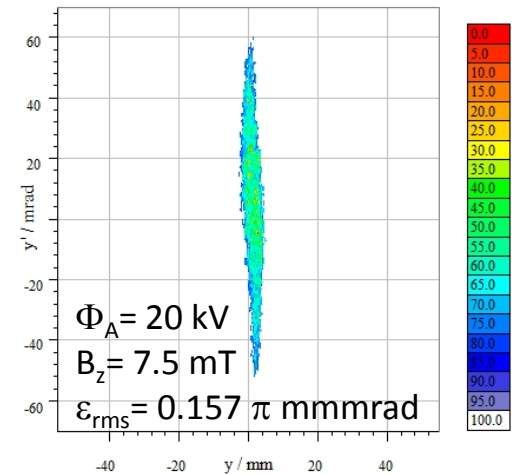


# 3.3. Low Current Measurements

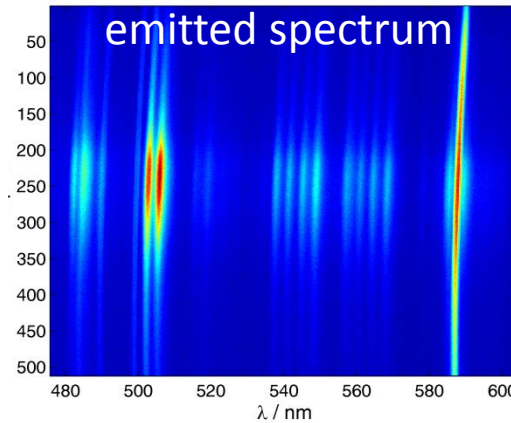
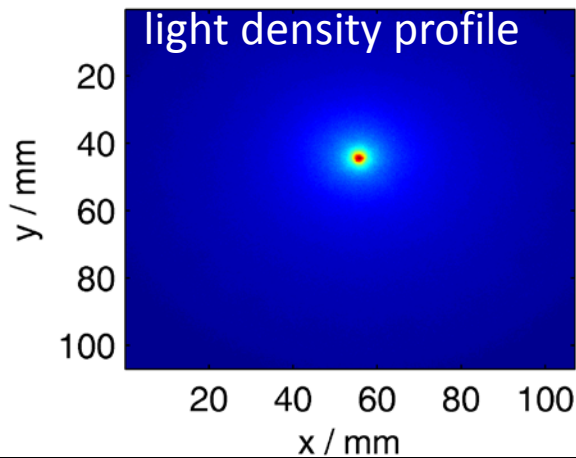
beam transport measurement



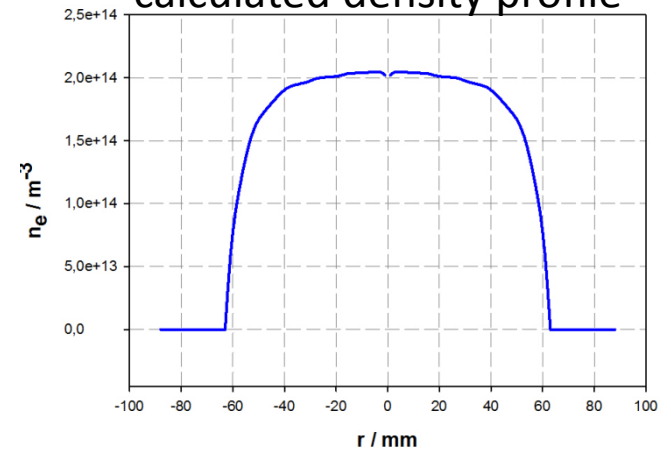
numerical simulation



NNP diagnostics



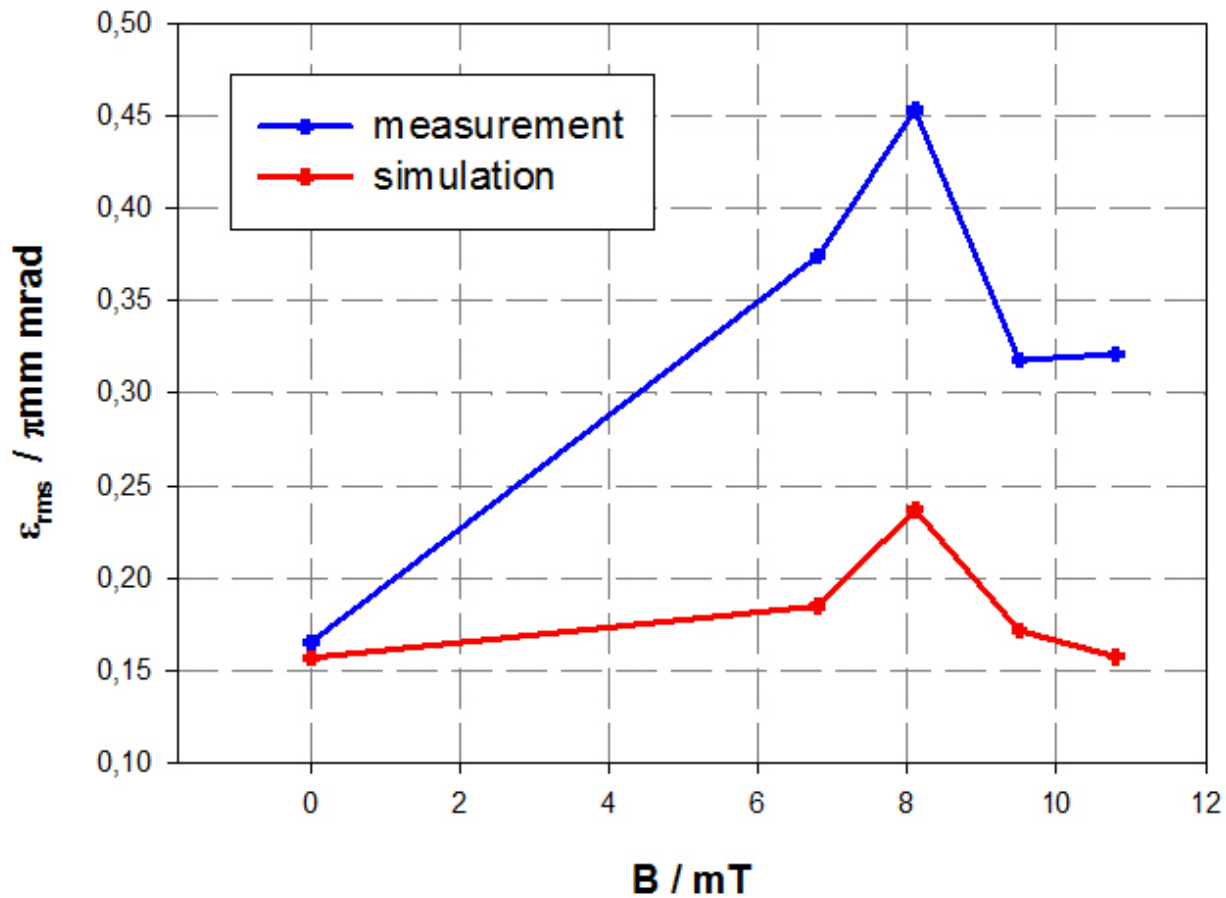
calculated density profile





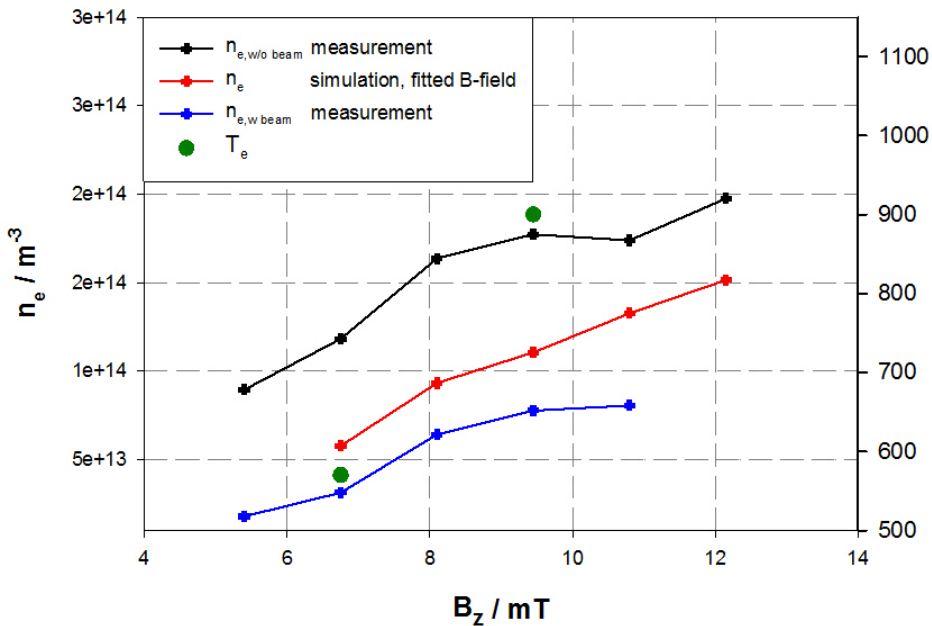
### 3.3. Low Current Measurements

comparison of measured and calculated rms-emittance

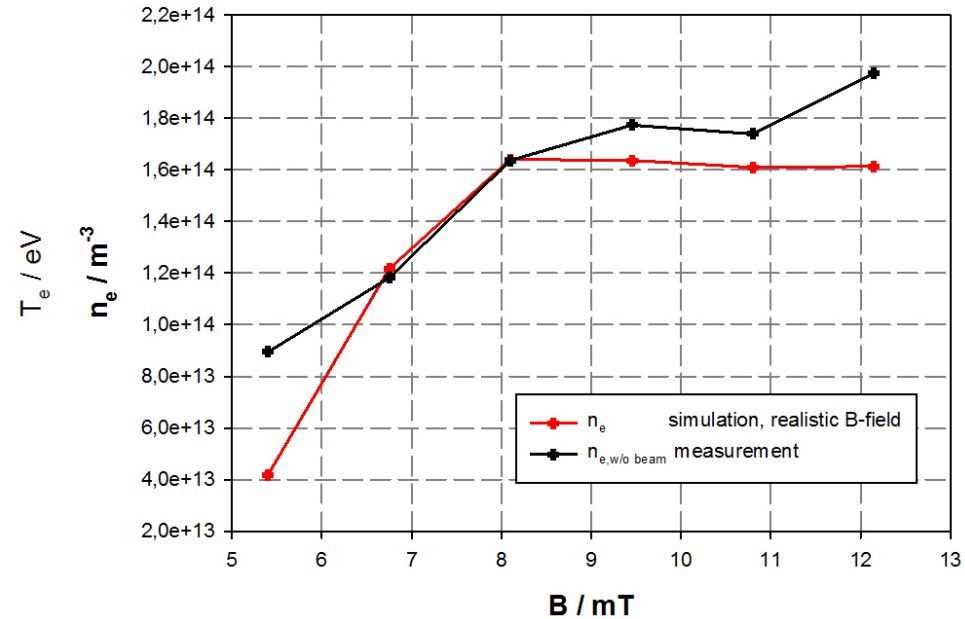


# 3.3. Low Current Measurements - Electron Density

comparison of calculated and measured electron densities as well as the measured electron temperature



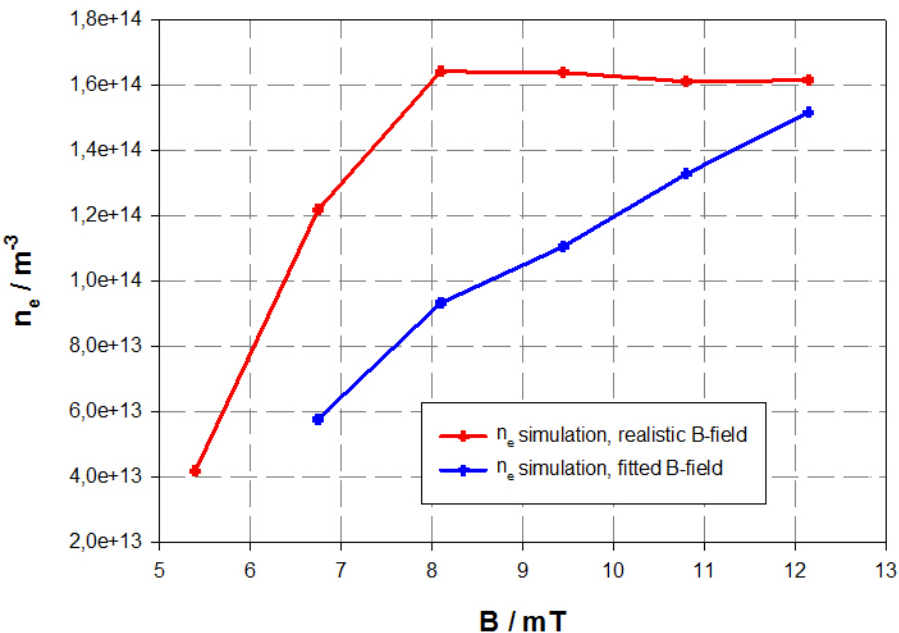
measured electron density in comparison with calculated electron density for realistic field configuration of Gabor lens



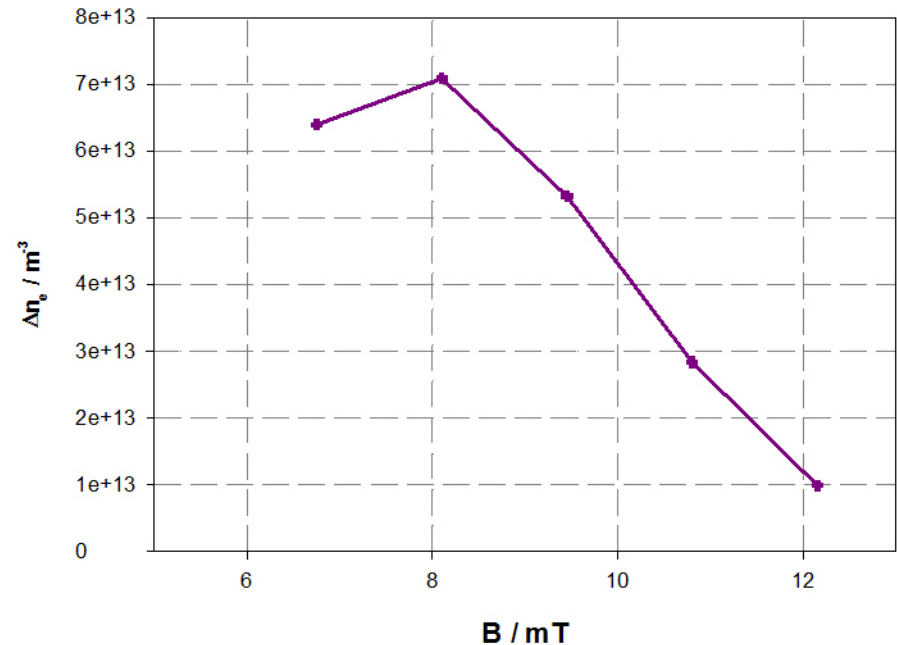
*preliminary results for electron temperature measurement as discussed before*

### 3.3. Low Current Measurements

comparison of calculated electron densities



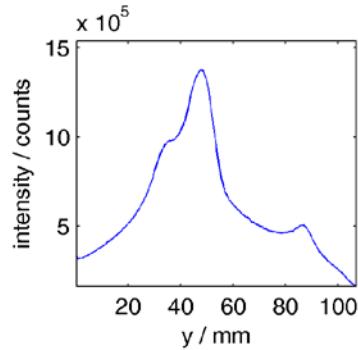
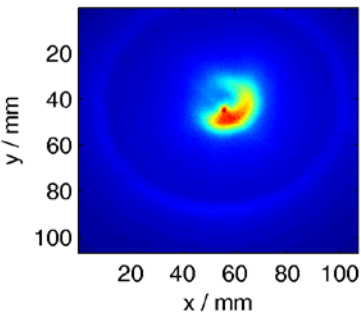
"missing" electron density



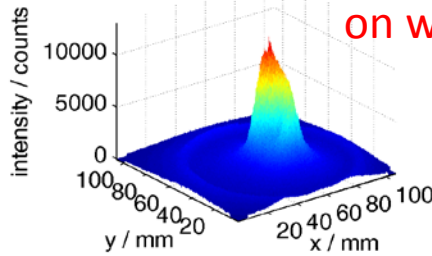
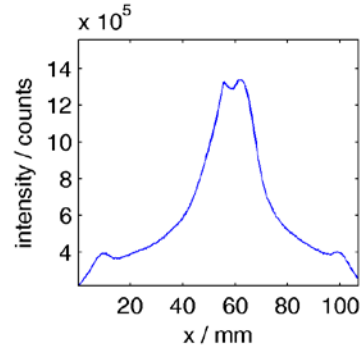
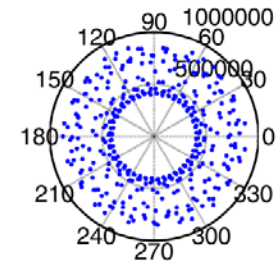
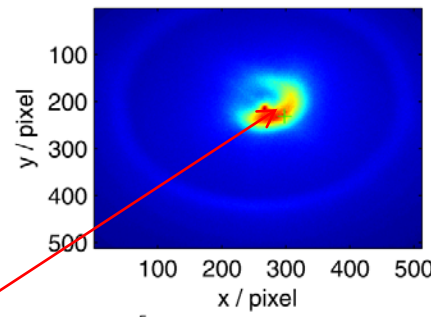
Because of this result another evaluation of the studies on NNP "without beam" in comparison with numerical simulation calculated with *realistic field configuration* of Gabor lens has been made.

# 3.3. Low Current Measurements

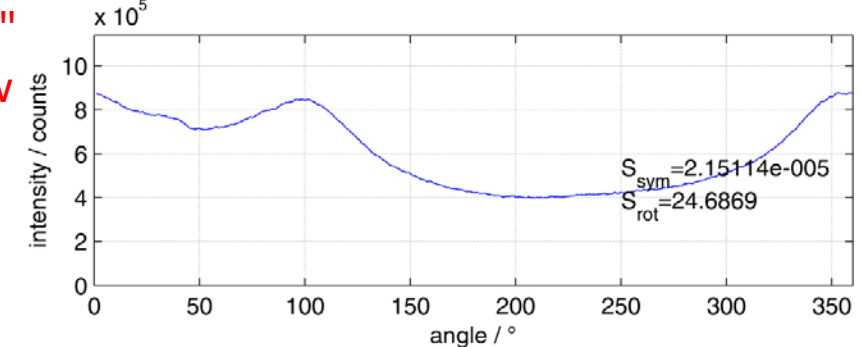
light density profile



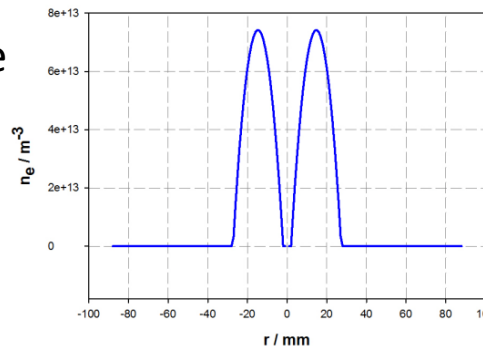
symmetry of plasma cloud



"light spot"  
 on window



calculated electron density profile



parameter setup:

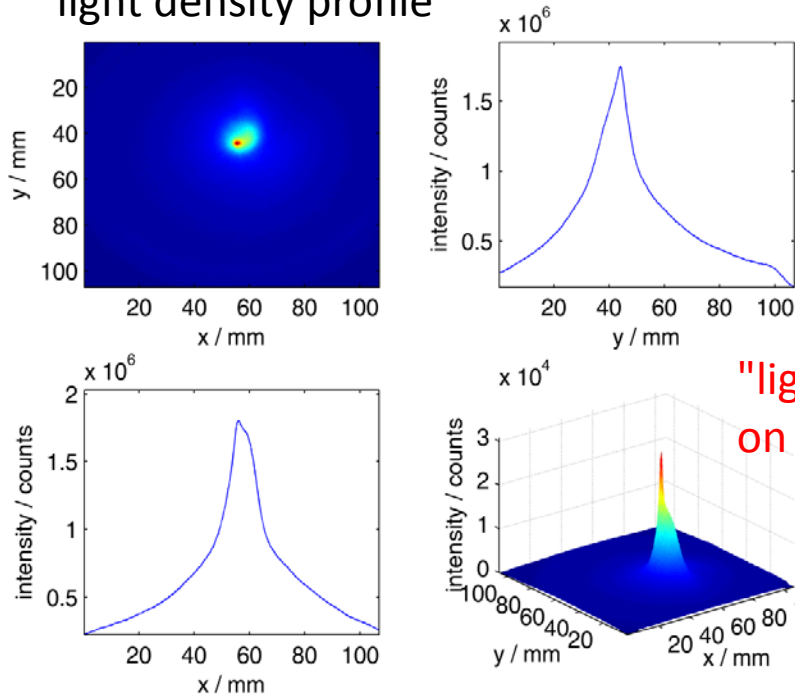
$\Phi_A = 20$  kV

$B_z = 5.4$  mT

$P = 9.6e-6$  (He)

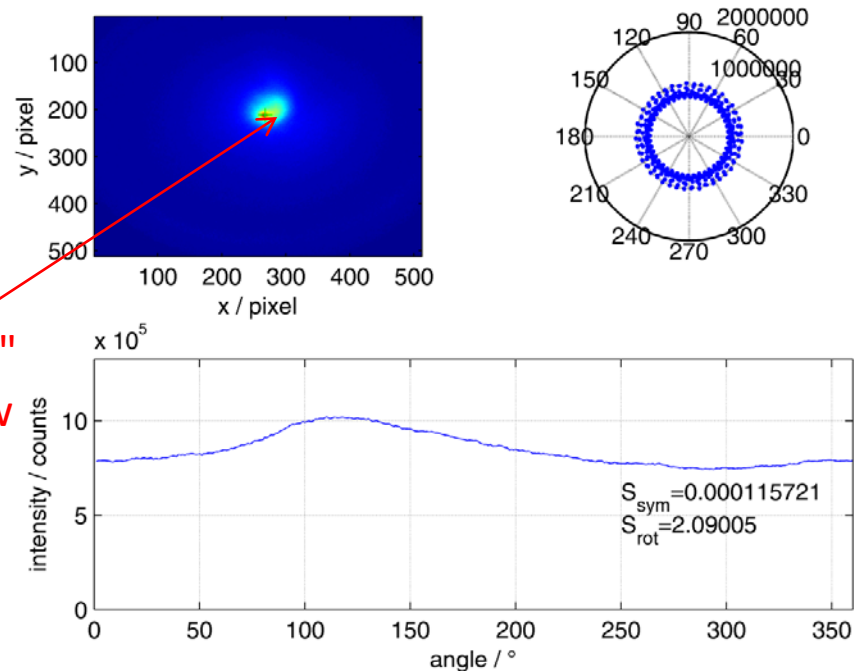
# 3.3. Low Current Measurements

light density profile

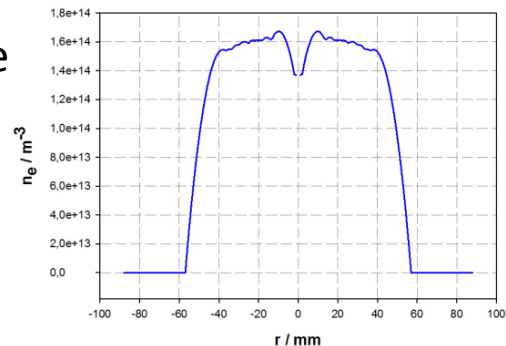


"light spot"  
 on window

symmetry of plasma cloud



calculated electron density profile

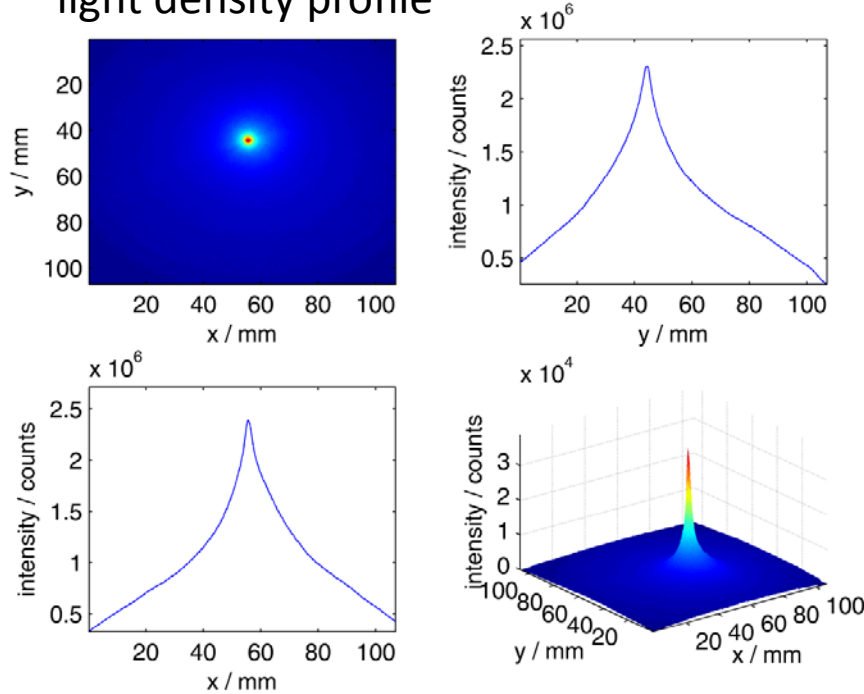


parameter setup:

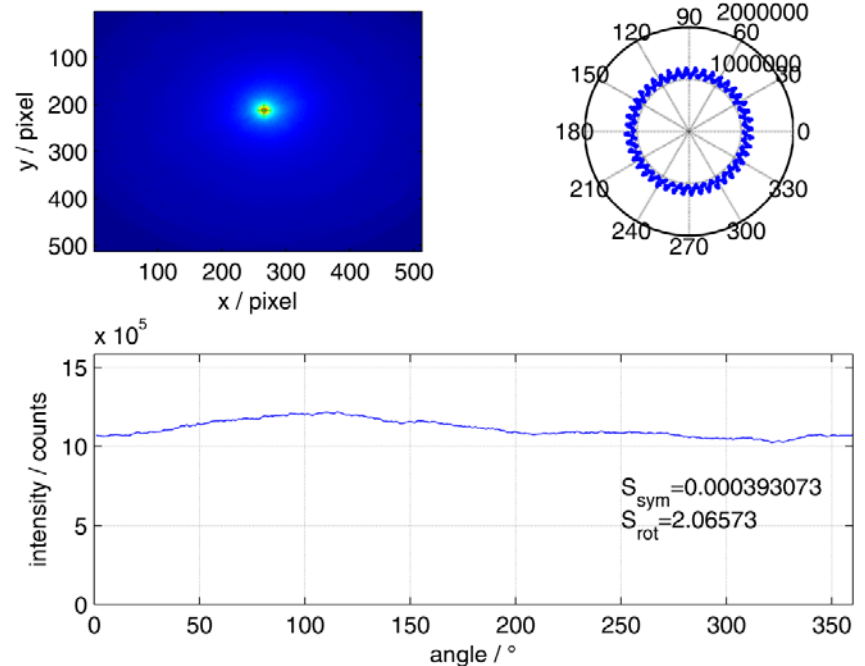
- $\Phi_A = 20$  kV
- $B_z = 6.8$  mT
- $P = 9.6e-6$  (He)

# 3.3. Low Current Measurements

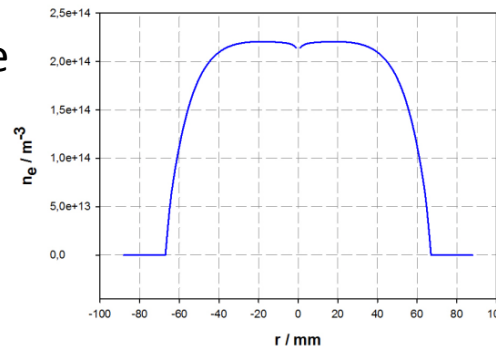
light density profile



symmetry of plasma cloud



calculated electron density profile

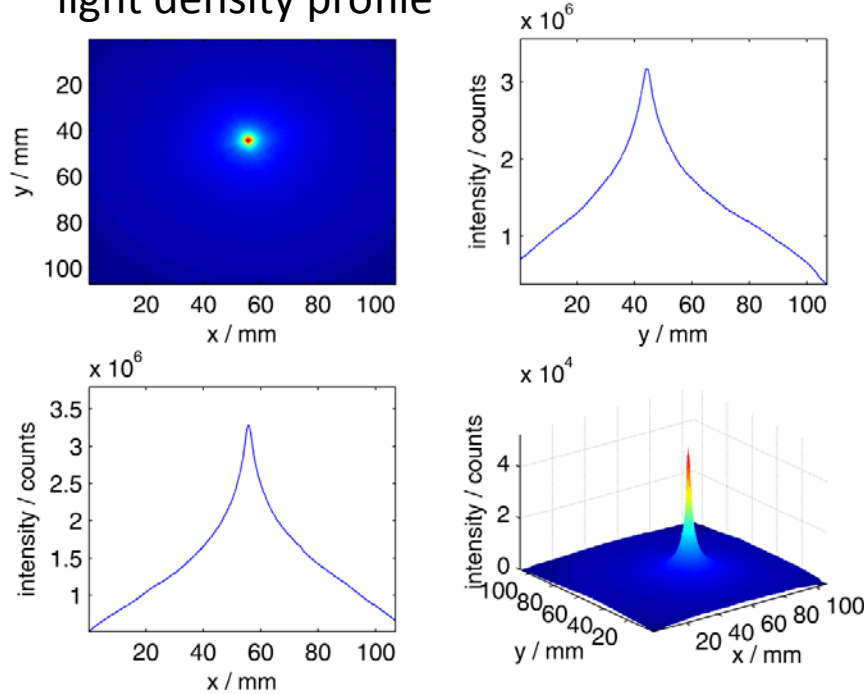


parameter setup:

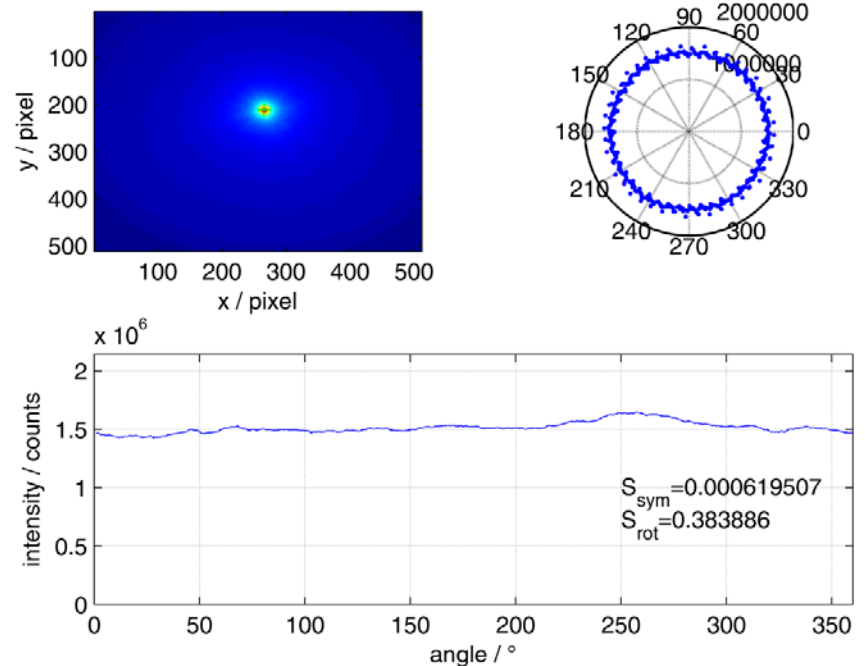
$\Phi_A = 20$  kV  
 $B_z = 8.1$  mT  
 $P = 9.6 \times 10^{-6}$  (He)

# 3.3. Low Current Measurements

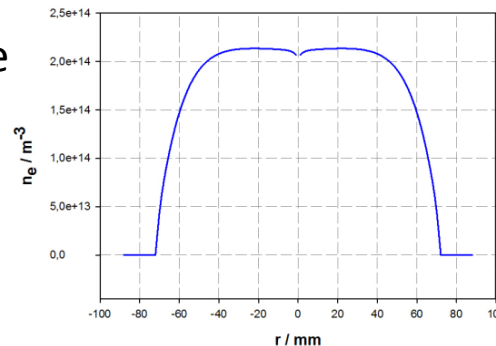
light density profile



symmetry of plasma cloud



calculated electron density profile

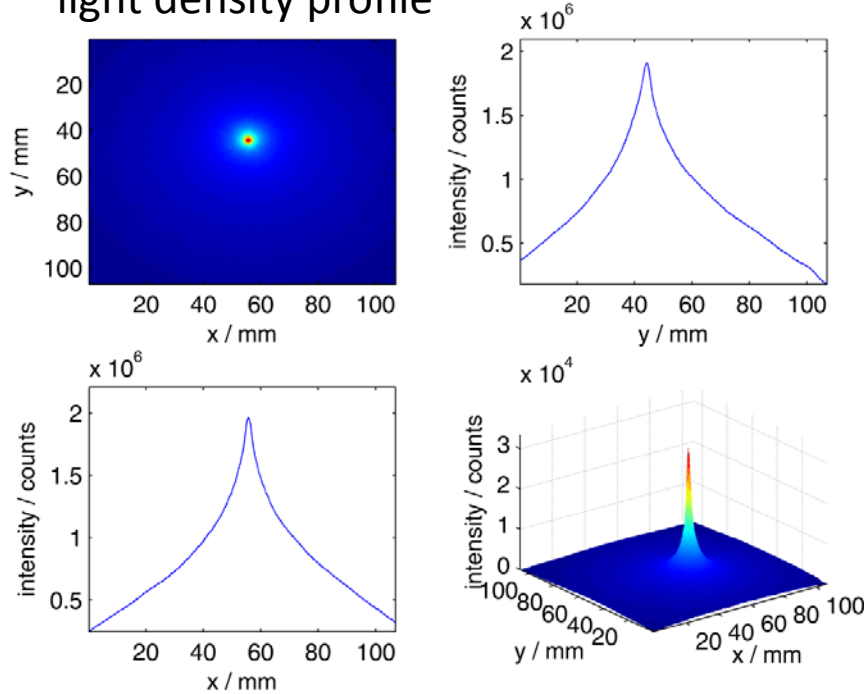


parameter setup:

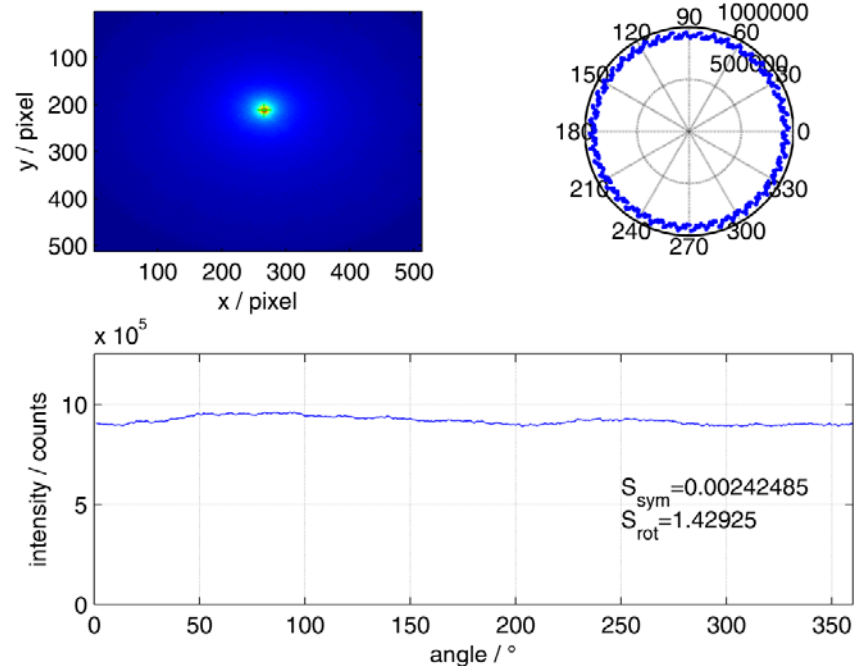
$\Phi_A = 20$  kV  
 $B_z = 9.5$  mT  
 $P = 9.6 \times 10^{-6}$  (He)

# 3.3. Low Current Measurements

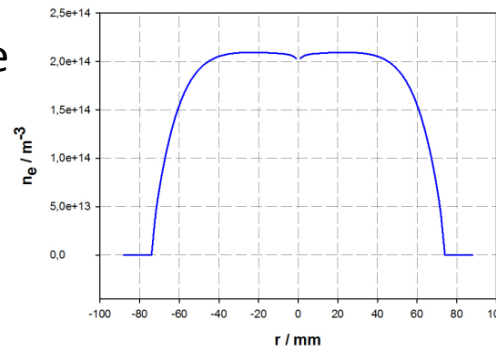
light density profile



symmetry of plasma cloud



calculated electron density profile



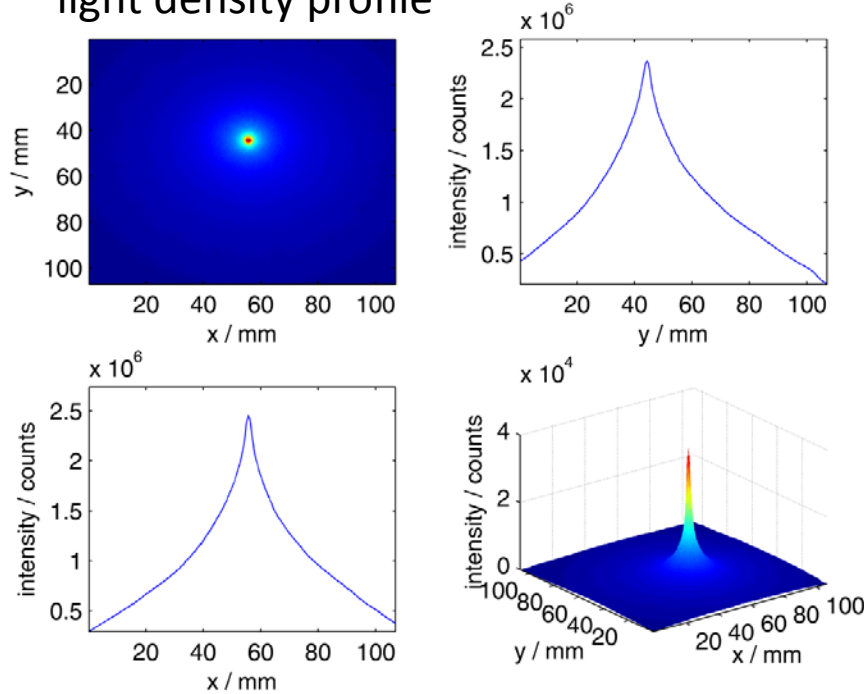
parameter setup:

$\Phi_A = 20$  kV  
 $B_z = 10.8$  mT  
 $P = 9.6 \times 10^{-6}$  (He)

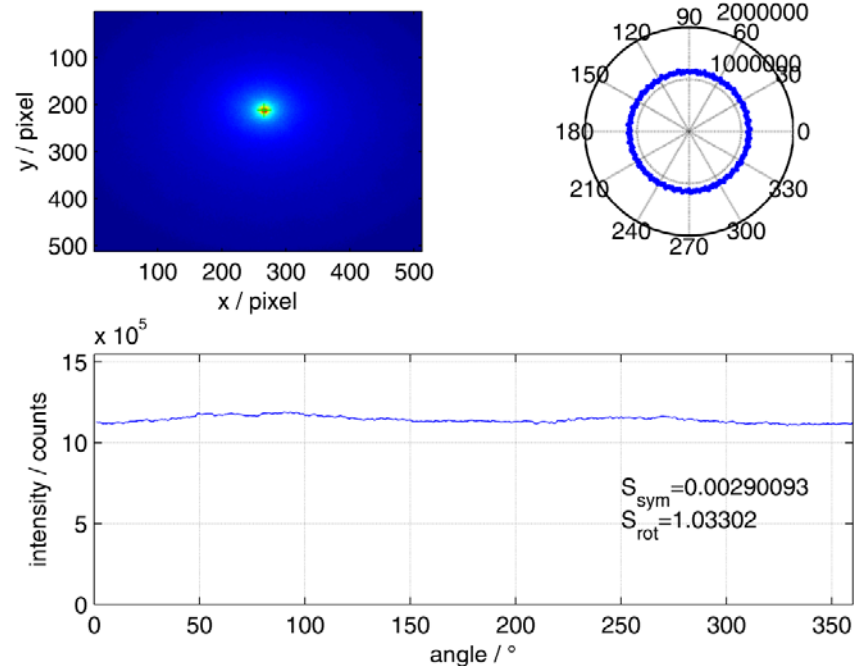


# 3.3. Low Current Measurements

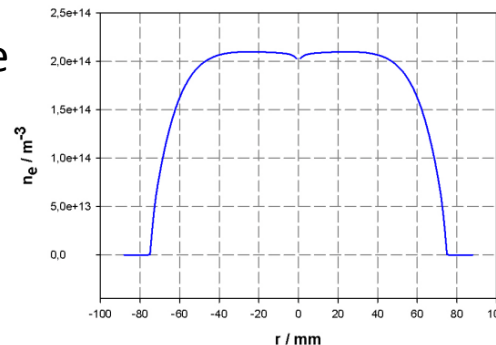
light density profile



symmetry of plasma cloud



calculated electron density profile

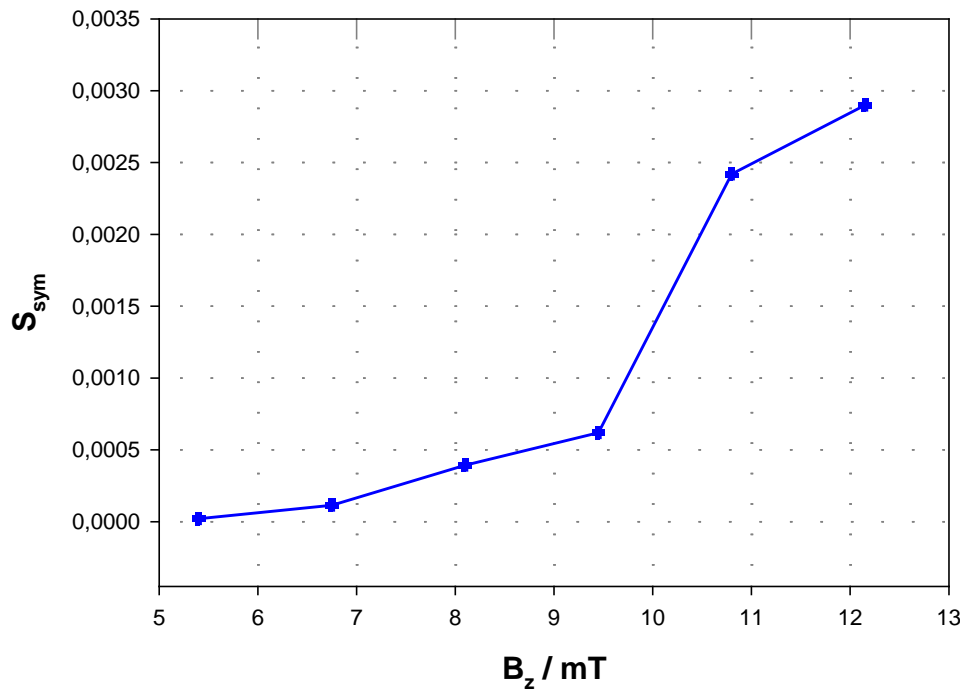


parameter setup:

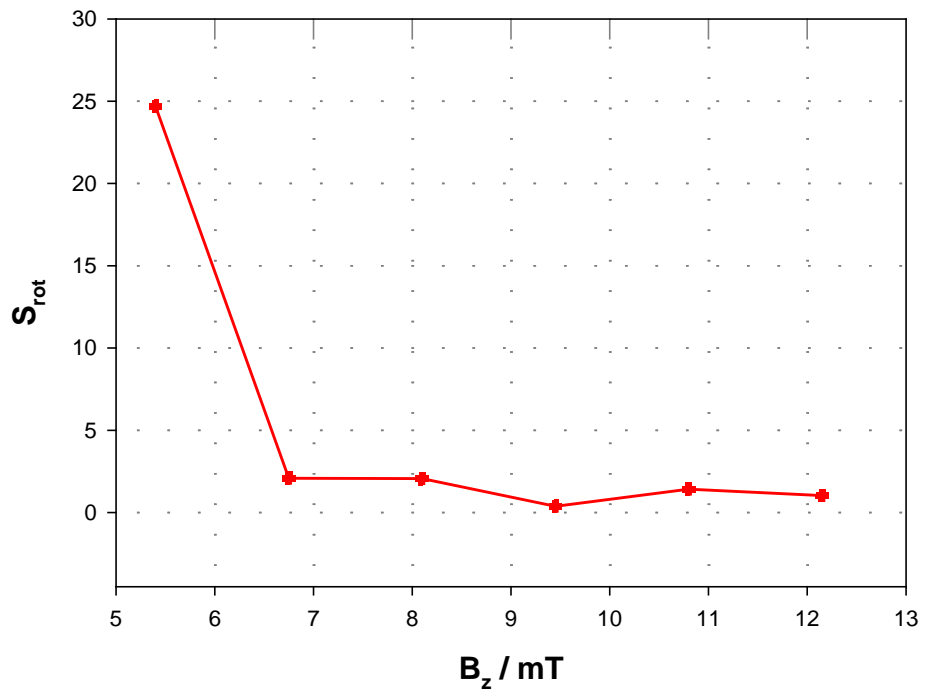
$\Phi_A = 20$  kV  
 $B_z = 12.2$  mT  
 $P = 9.6 \times 10^{-6}$  (He)

### 3.3. Low Current Measurements

symmetry

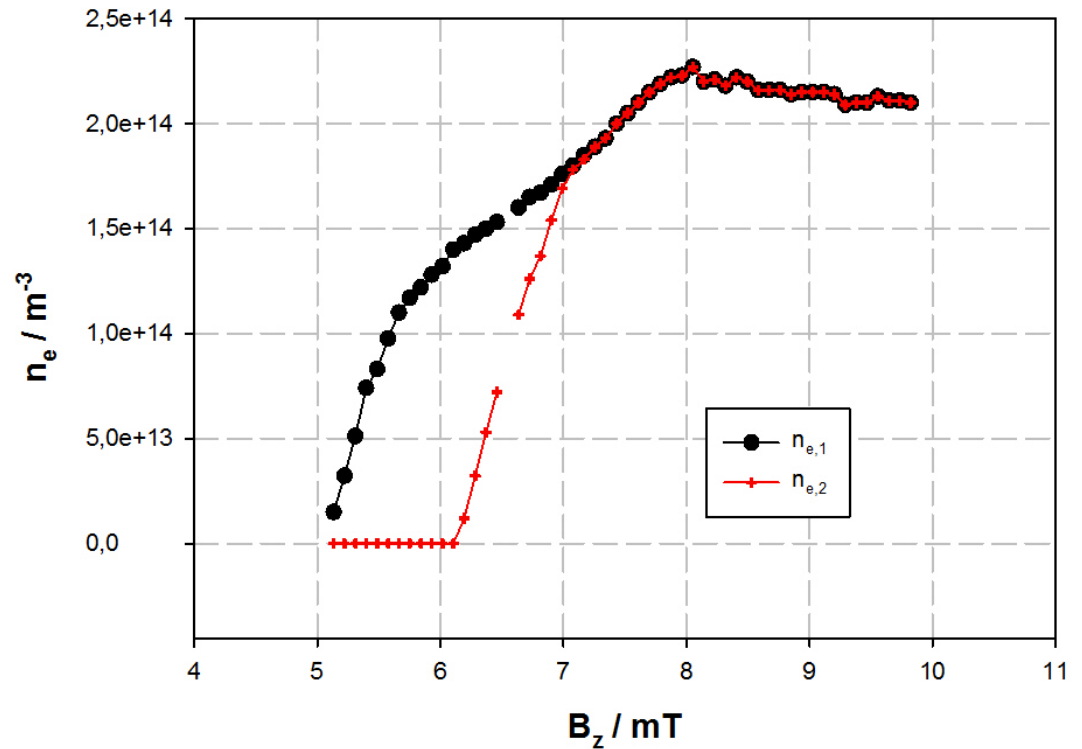


rotational symmetry



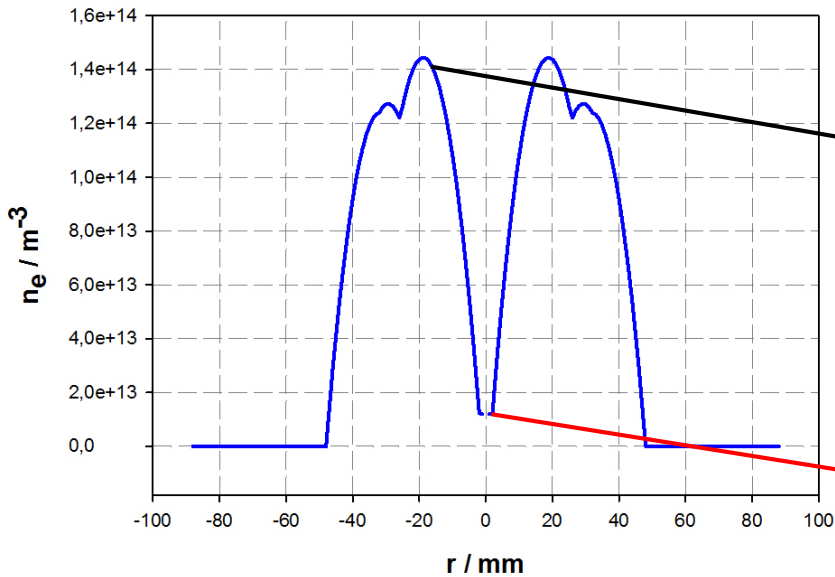
### 3.3. Low Current Measurements

simulated maximum electron density

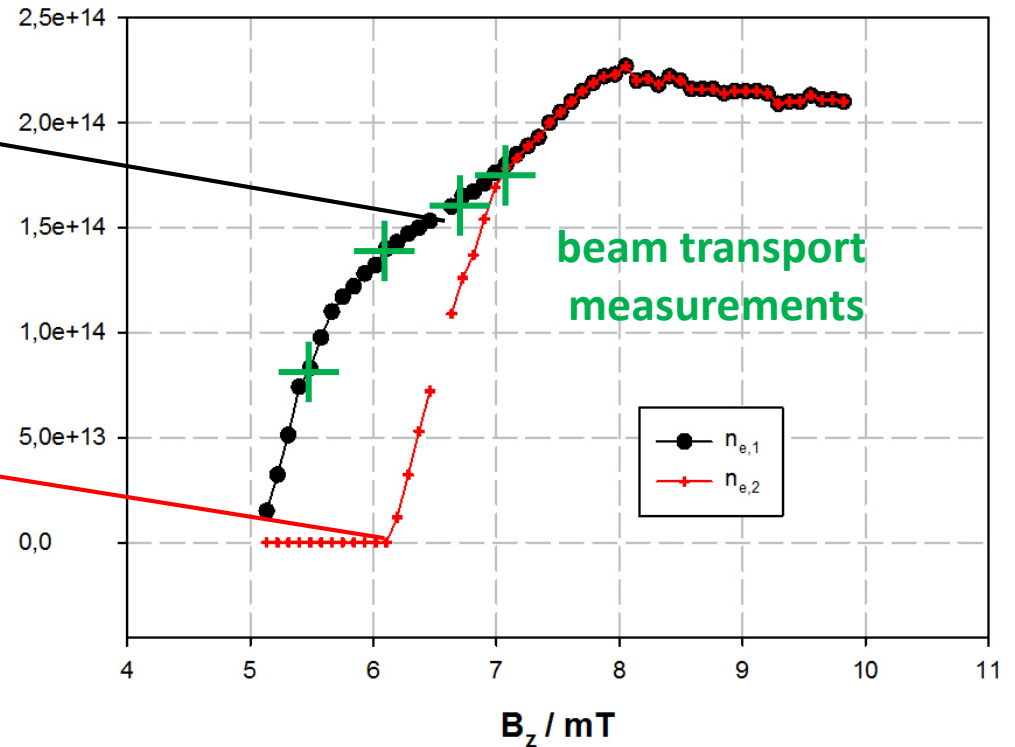


# 3.3. Low Current Measurements

simulated electron density distribution

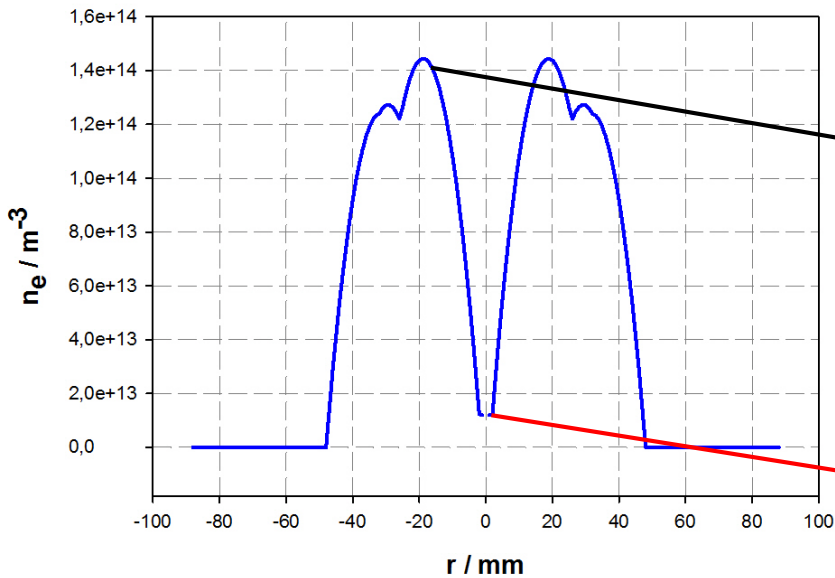


simulated maximum electron density

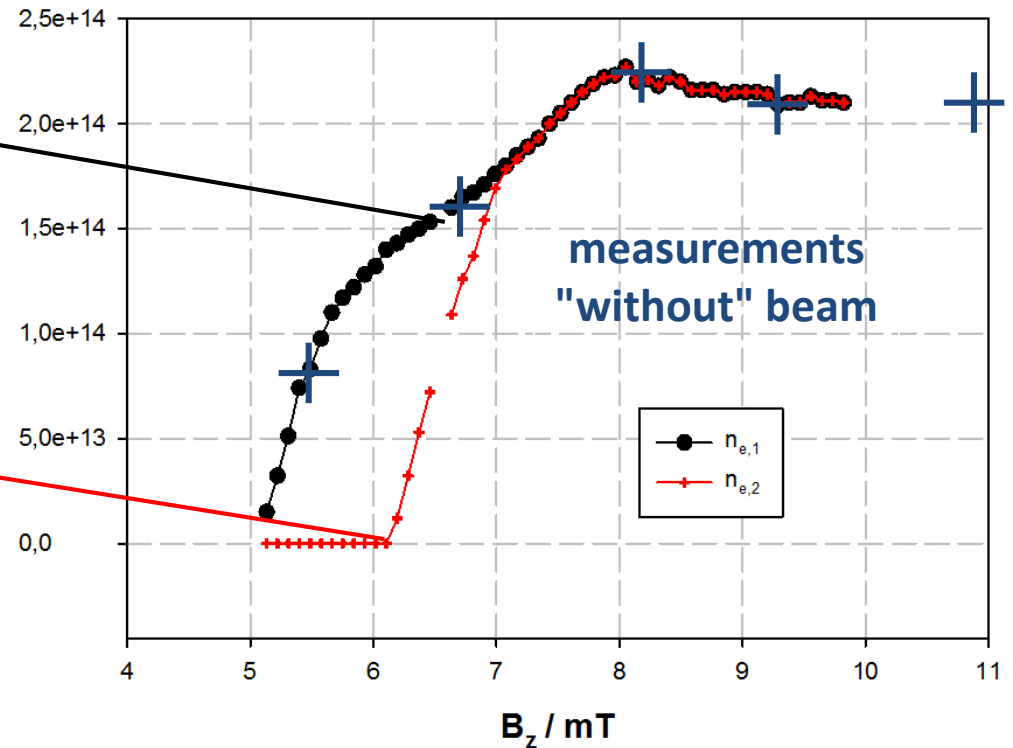


### 3.3. Low Current Measurements

simulated electron density distribution



simulated maximum electron density

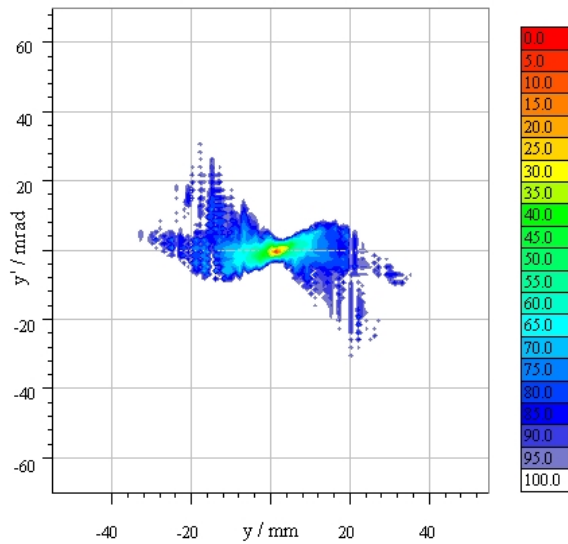


carefully asking: *beam-driven instability?!*

## 3.4. High Current Measurements - e<sup>-</sup> Production

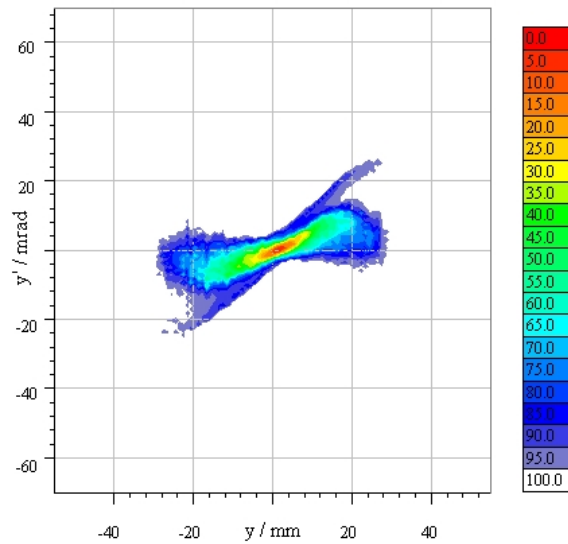
Influence of ion beam current / electron production rate on focusing strength ?!

$$\frac{n_i}{n_e} = 0,07$$



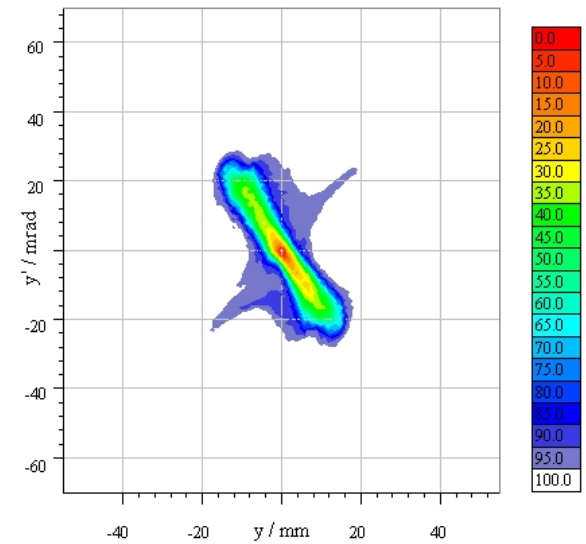
$I_B=5$  mA

$$\frac{n_i}{n_e} = 0,20$$



$I_B=15$  mA

$$\frac{n_i}{n_e} = 0,26$$



$I_B=20$  mA

lens parameters:

$$\Phi_A = 9.5 \text{ kV}$$

$$B_z = 9.7 \text{ mT}$$

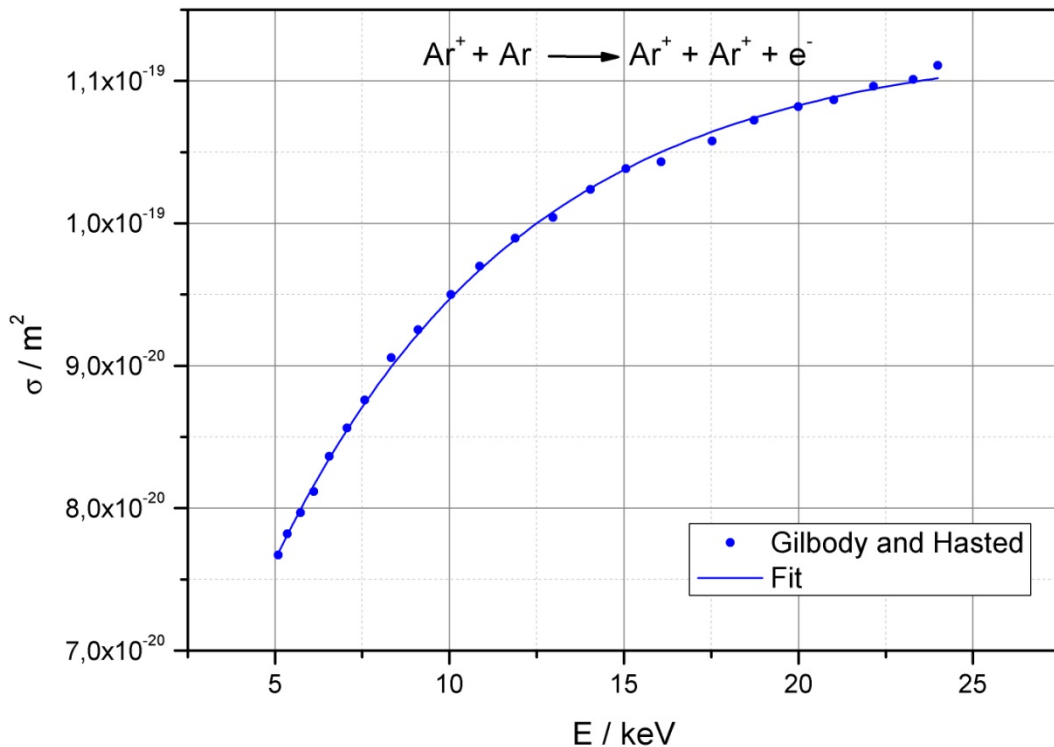
beam parameters:

Ar<sup>+</sup>

$$W_B = 88 \text{ keV (2.2 keV/u)}$$

# 3.4. High Current Measurements - e<sup>-</sup> Production

## Ionization Cross Section



$I_B = 5 \text{ mA} \rightarrow n_i = 2.45 \cdot 10^{13} \text{ m}^{-3}$ :  
 $v_{in} = n_n \sigma(24\text{keV}) v_i = 2161 \text{ Hz}$   
 $dn/dt = v_{in} n_i = 5.3 \cdot 10^{16} \text{ m}^{-3}\text{s}^{-1}$

-->  **$6.61 \cdot 10^{13} \text{ m}^{-3}$**  within 1.25 ms

$I_B = 15 \text{ mA} \rightarrow n_i = 7.35 \cdot 10^{13} \text{ m}^{-3}$ :  
 $dn/dt = v_{in} n_i = 1.59 \cdot 10^{17} \text{ m}^{-3}\text{s}^{-1}$

-->  **$2 \cdot 10^{14} \text{ m}^{-3}$**  within 1.25 ms

$I_B = 20 \text{ mA} \rightarrow n_i = 9.81 \cdot 10^{13} \text{ m}^{-3}$ :  
 $dn/dt = v_{in} n_i = 2.12 \cdot 10^{17} \text{ m}^{-3}\text{s}^{-1}$

-->  **$2.65 \cdot 10^{14} \text{ m}^{-3}$**  within 1.25 ms

### beam parameters:

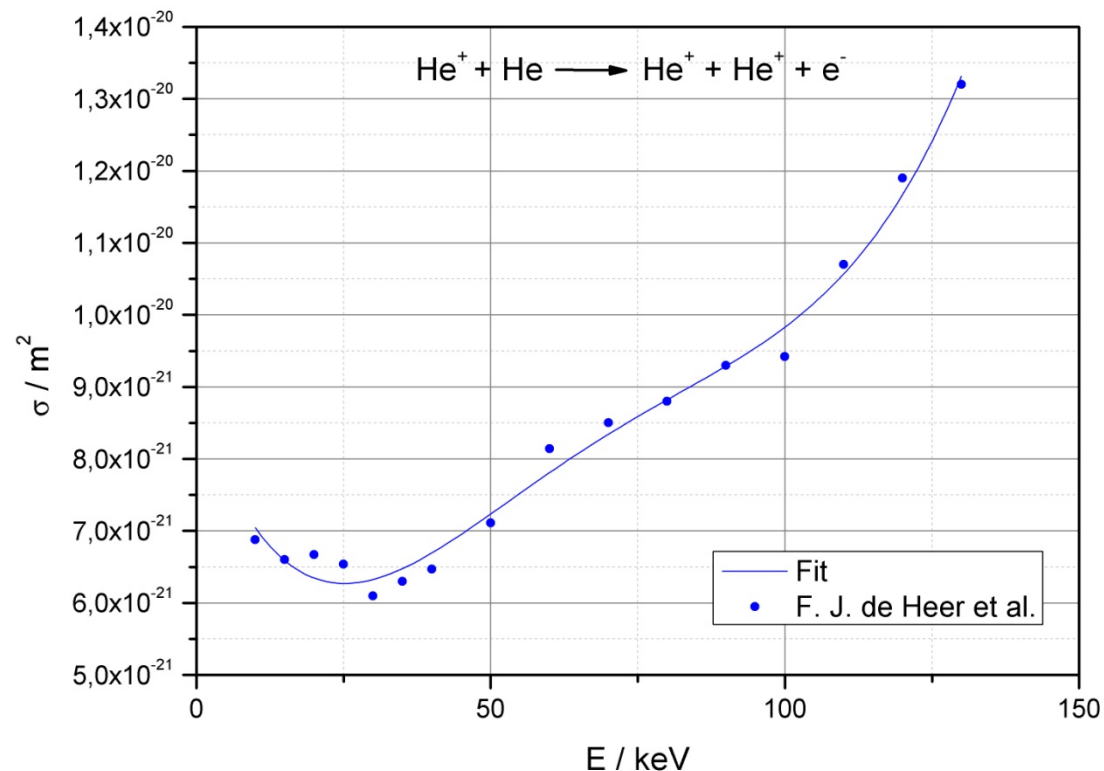
$\text{Ar}^+$ ,  $W_B = 88 \text{ keV}$  (2.2 keV/u) -->  $v_i = 650 \cdot 10^3 \text{ m/s}$

### lens parameters:

$\Phi_A = 9.5 \text{ kV}$ ,  $B_z = 9.7 \text{ mT}$ ,  $n_{e,\text{theo,max}} = 3.9 \cdot 10^{14} \text{ m}^{-3}$ ,  
 $n_{e,\text{simu,max}} = 1.15 \cdot 10^{14} \text{ m}^{-3}$

# 3.4. High Current Measurements - e<sup>-</sup> Production

## Ionization Cross Section



Comparison:

$I_B = 3 \text{ mA} \rightarrow n_i = 4.84 \cdot 10^{12} \text{ m}^{-3}$ :  
 $v_{in} = n_n \sigma(50 \text{ keV}) v_i = 2612 \text{ Hz}$   
 $dn/dt = v_{in} n_i = 1.26 \cdot 10^{16} \text{ m}^{-3}\text{s}^{-1}$   
 -->  **$1.58 \cdot 10^{13} \text{ m}^{-3}$**  within 1.25 ms

Other e<sup>-</sup> production processes like  
*secondary thermal ions on chamber wall (charge exchange)*  
 or  
*beam ions striking ground vessel*  
 are neglected.

### beam parameters:

He<sup>+</sup>,  $W_B = 50.3 \text{ keV}$  (12.6 keV/u) -->  $v_i = 1.6 \cdot 10^3 \text{ m/s}$

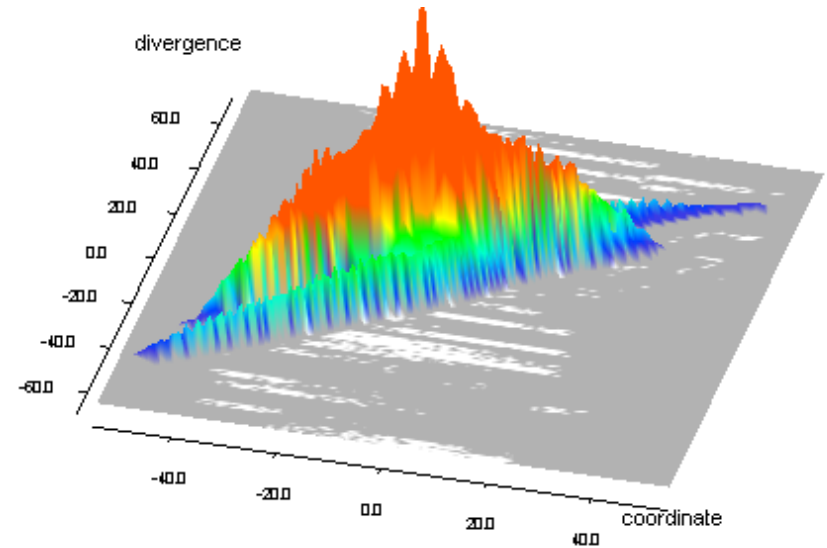
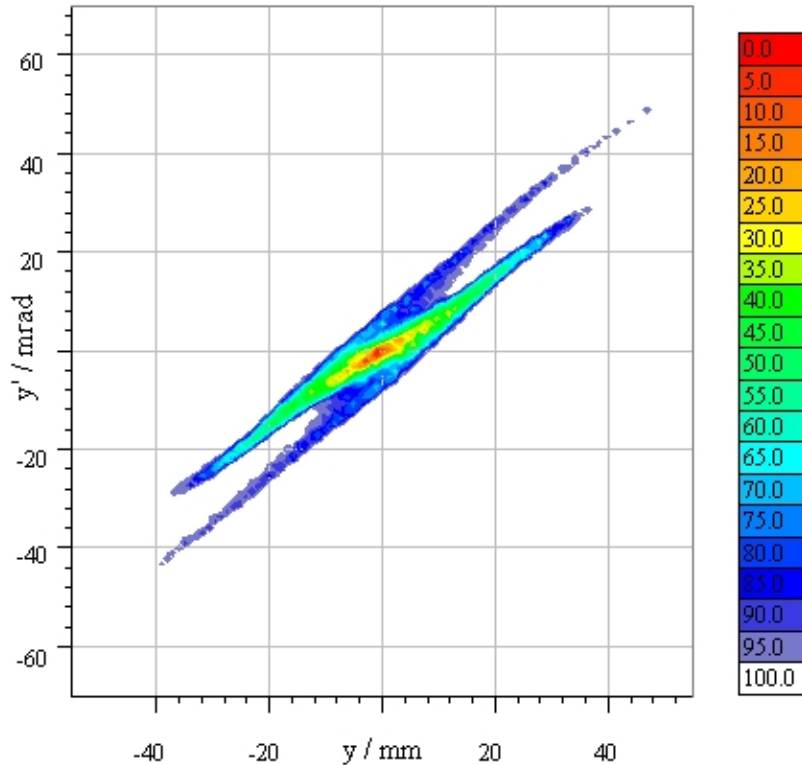
### lens parameters:

$\Phi_A = 20 \text{ kV}$ ,  $B_z = 12.2 \text{ mT}$ ,  $n_{e,theo,max} = 7.9 \cdot 10^{14} \text{ m}^{-3}$ ,  
 $n_{e,simu,max} = 2 \cdot 10^{14} \text{ m}^{-3}$



# 3.4. High Current Measurements

drifted beam

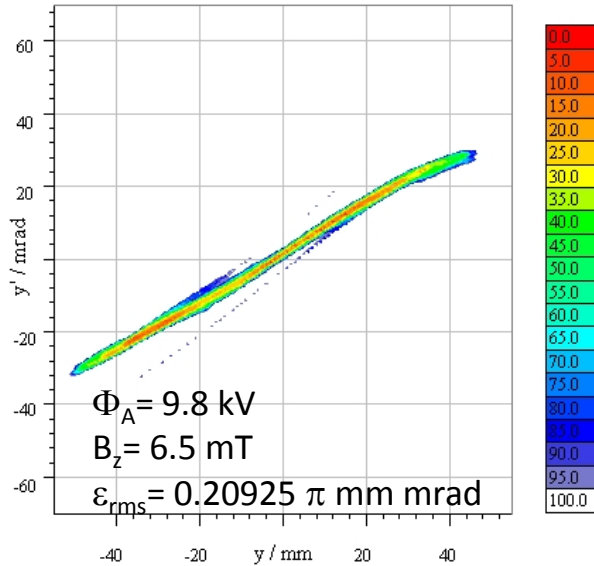


Ar<sup>+</sup>  
W<sub>b</sub> = 124 keV, 3.1 keV/u  
I<sub>B</sub> = 30 mA

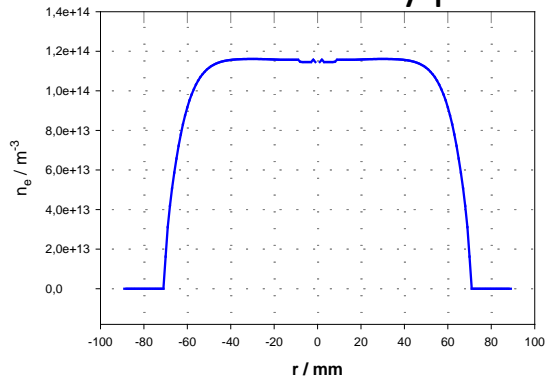
$\Phi_A = 0$  kV  
 $B_z = 0$  mT  
 $\epsilon_{100\%} = 1860.69$  mm mrad  
 $\epsilon_{97\%} = 269.8$  mm mrad  
 $\epsilon_{rms} = 0.16558 \pi$  mm mrad  
 $\omega = 3.45$   
 $n = 3$

# 3.4. High Current Measurements

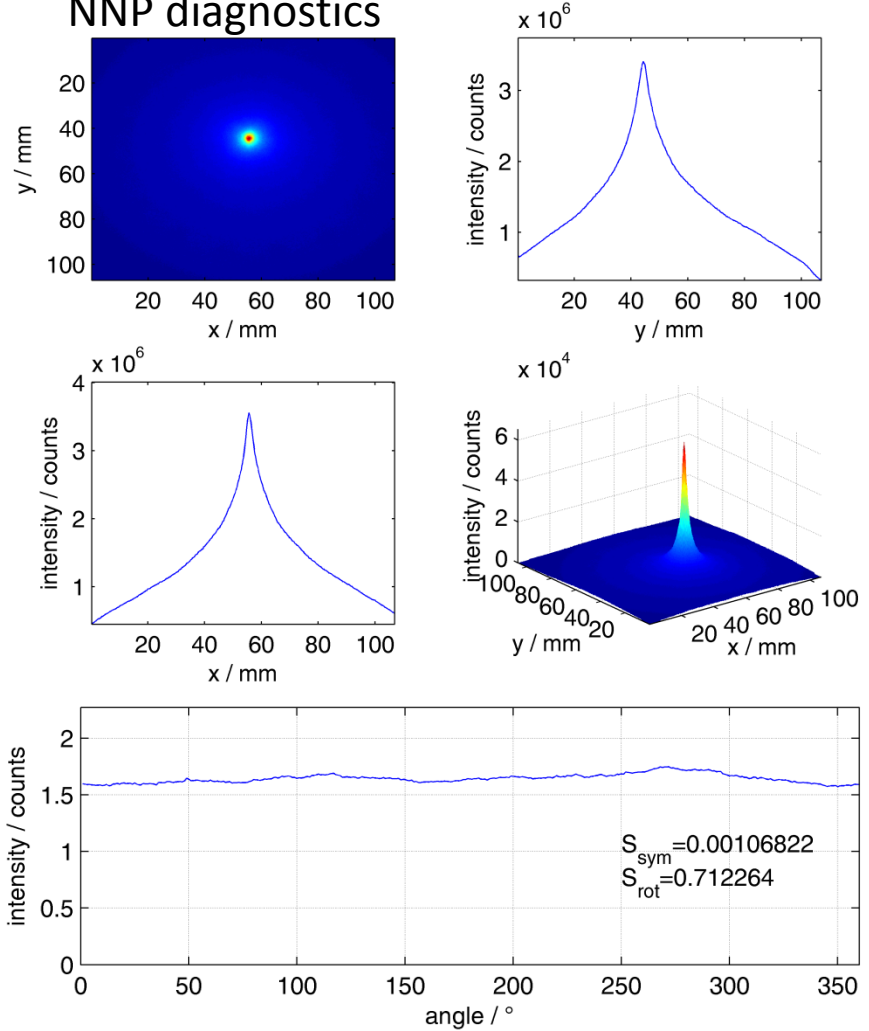
## beam transport measurement



## calculated density profile

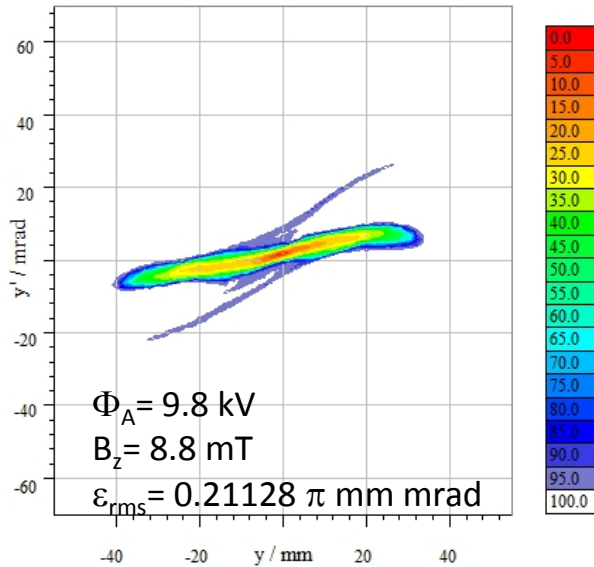


## NNP diagnostics

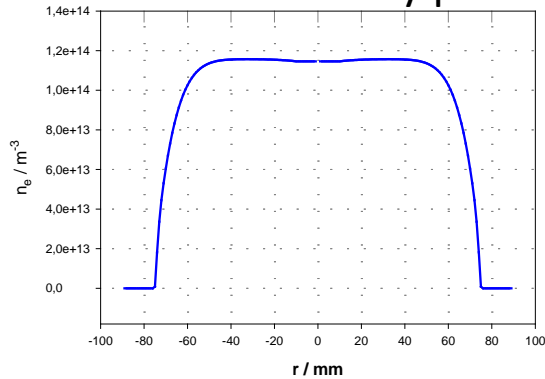


# 3.4. High Current Measurements

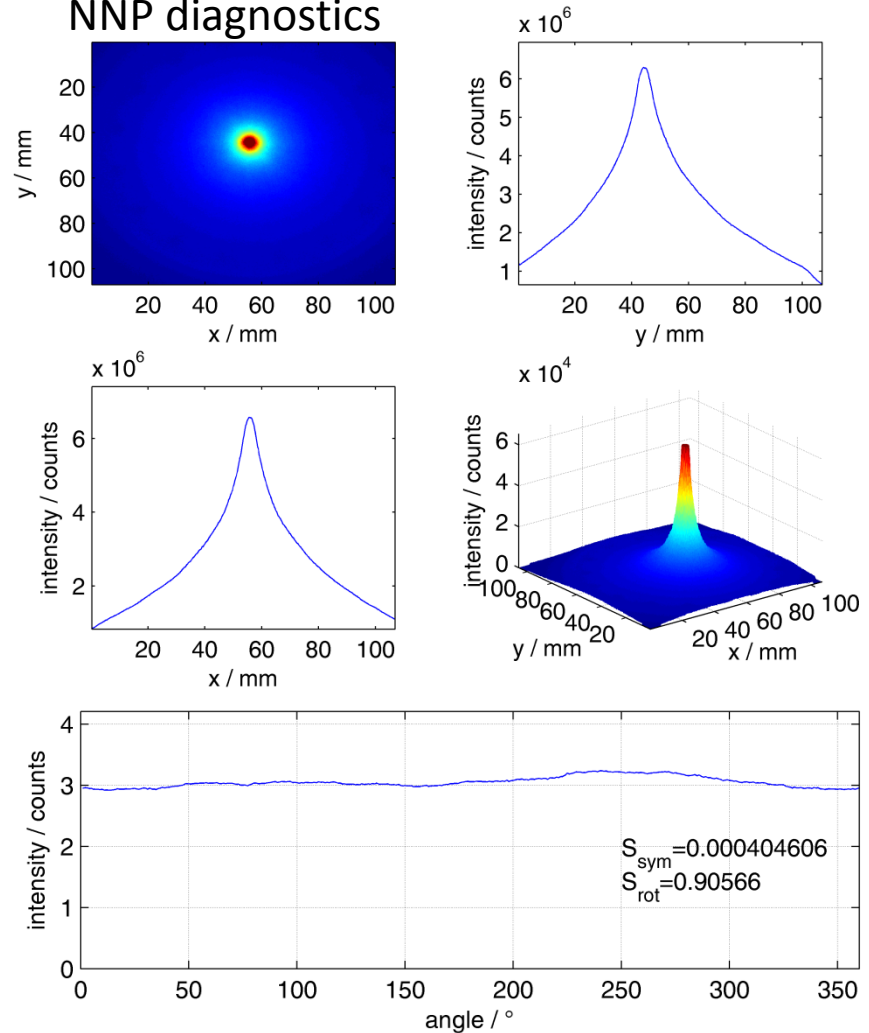
## beam transport measurement



## calculated density profile

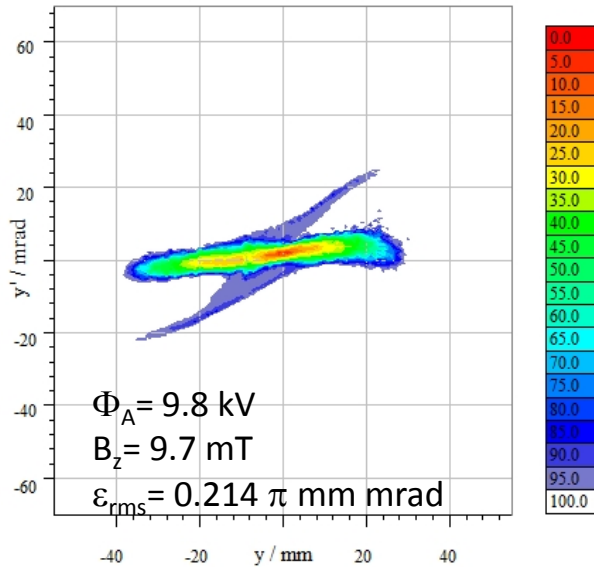


## NNP diagnostics

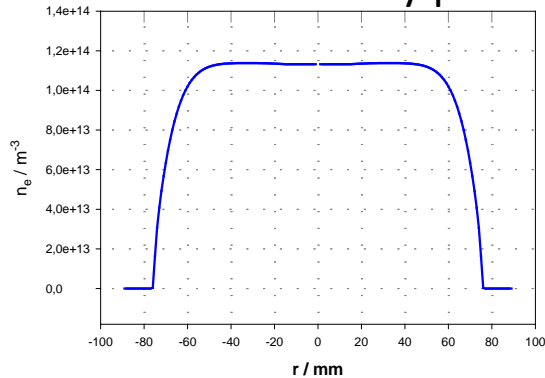


# 3.4. High Current Measurements

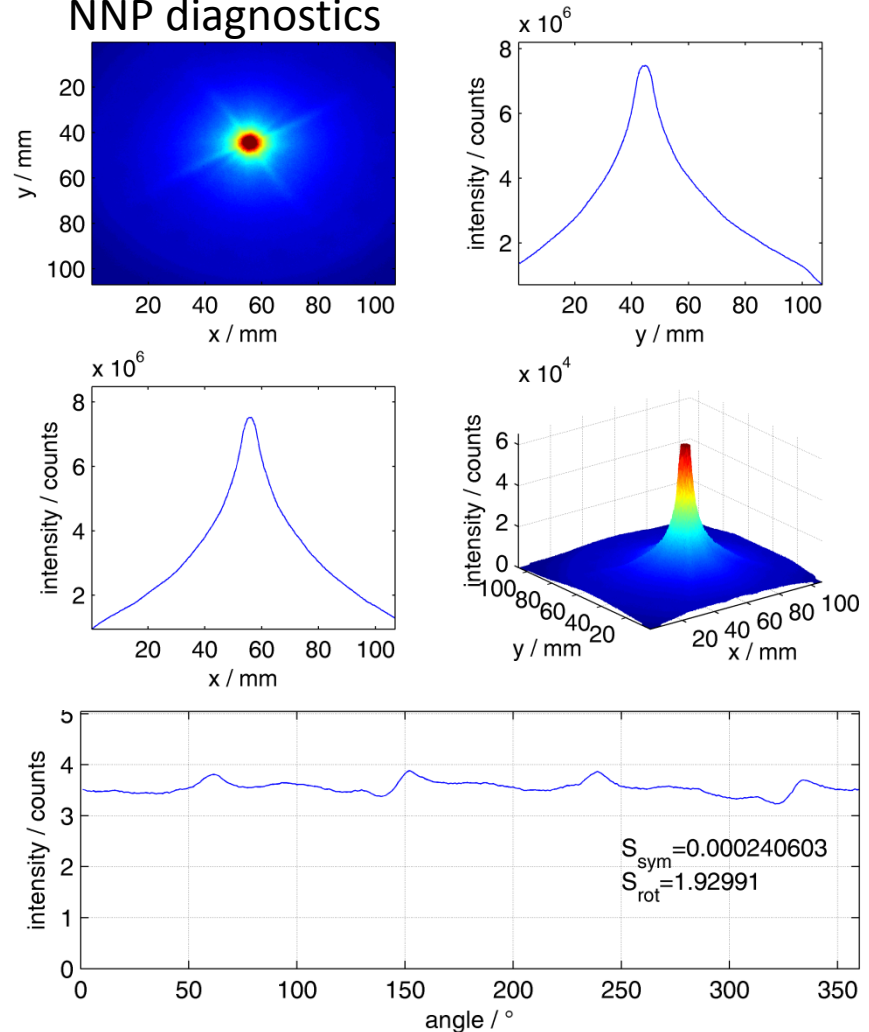
## beam transport measurement



## calculated density profile

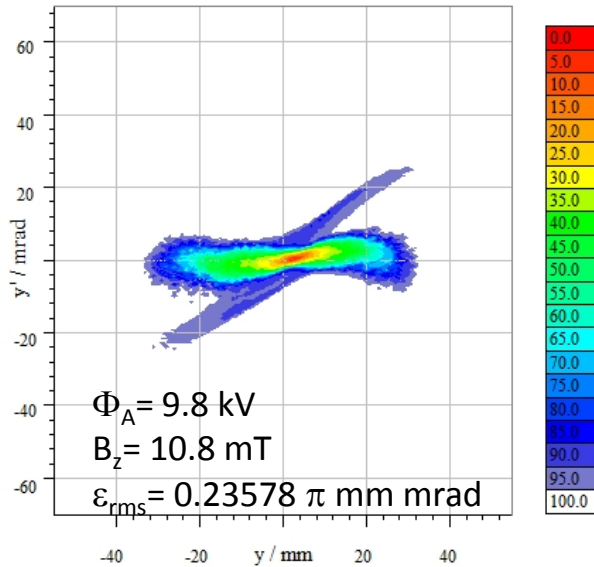


## NNP diagnostics

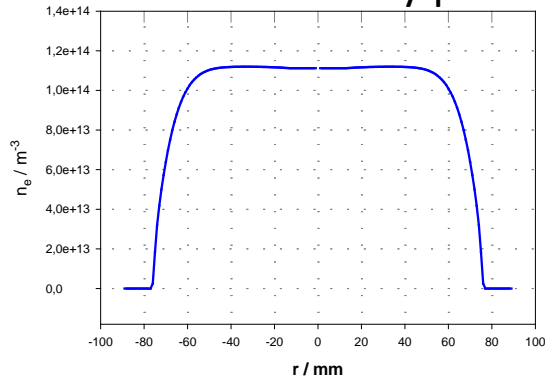


# 3.4. High Current Measurements

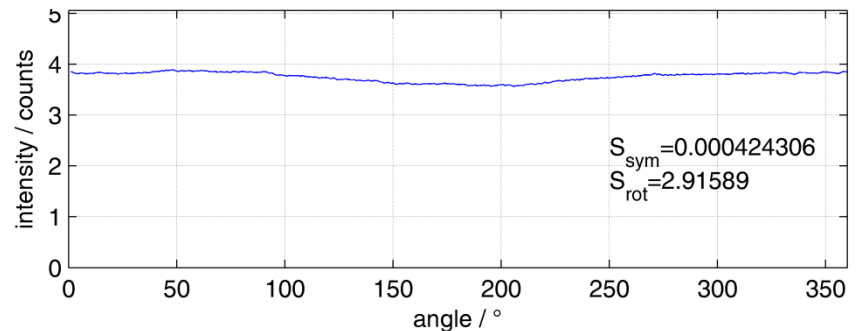
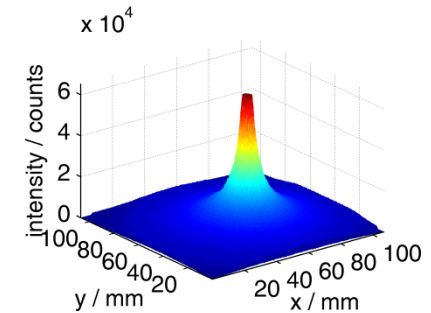
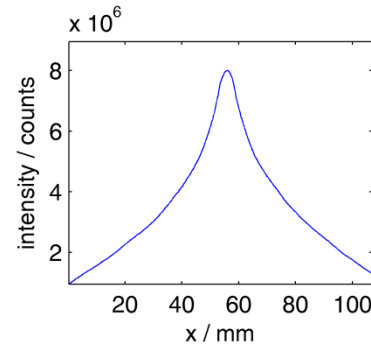
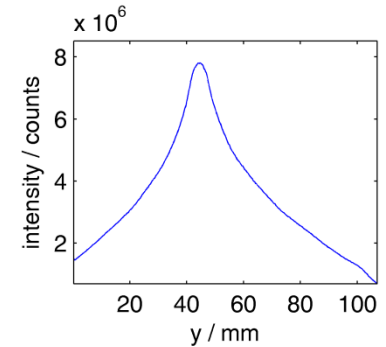
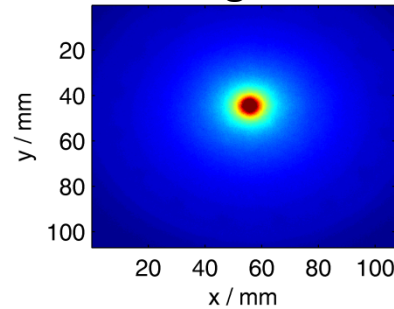
## beam transport measurement



## calculated density profile

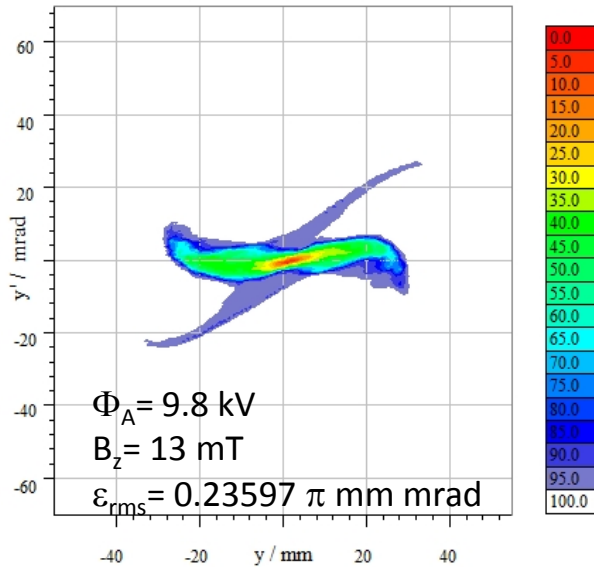


## NNP diagnostics

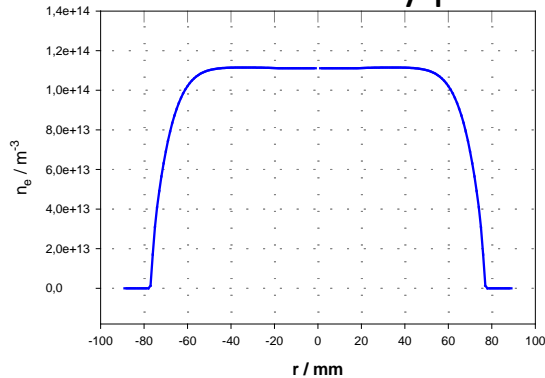


# 3.4. High Current Measurements

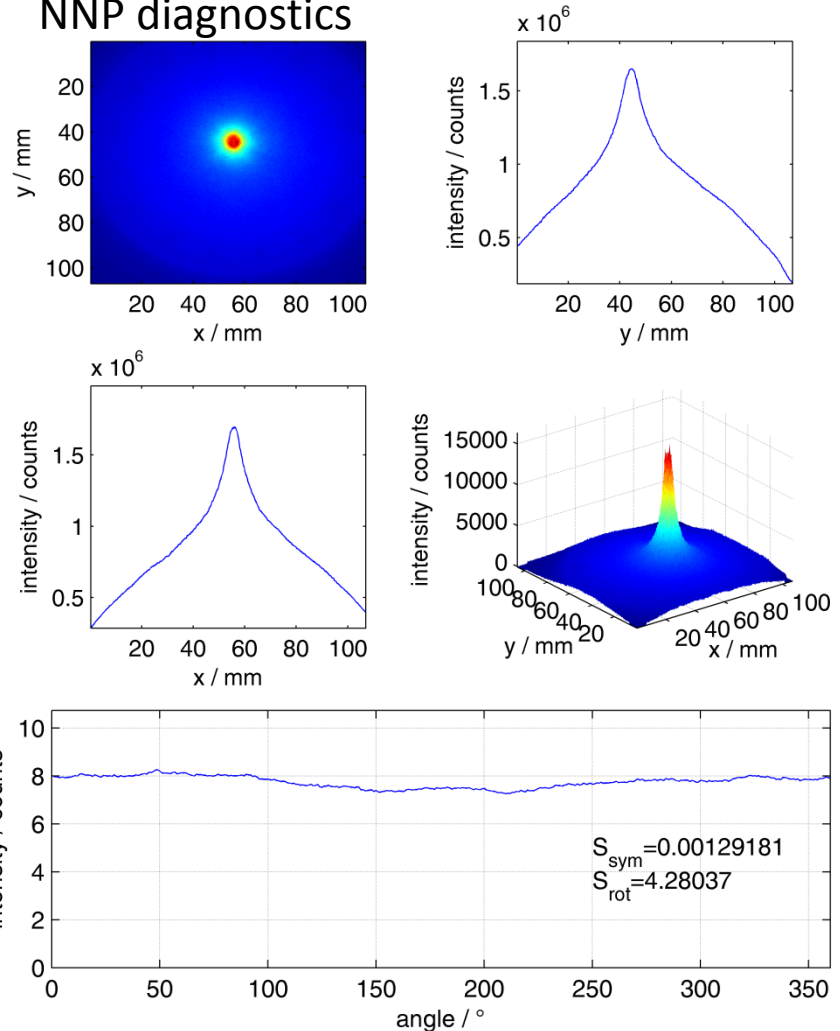
## beam transport measurement



## calculated density profile

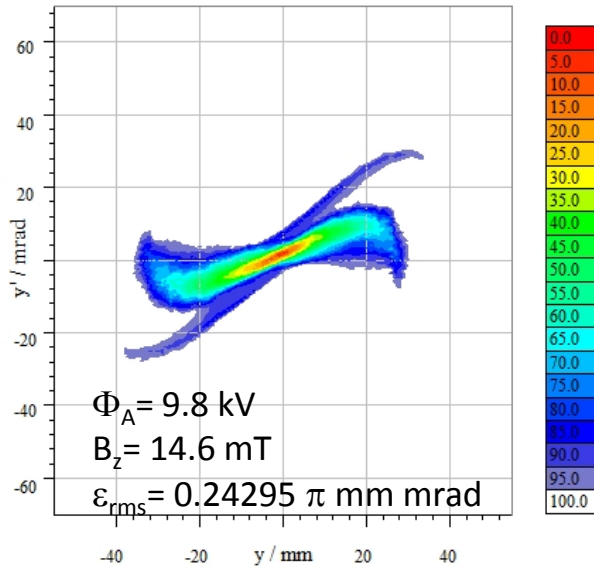


## NNP diagnostics



# 3.4. High Current Measurements

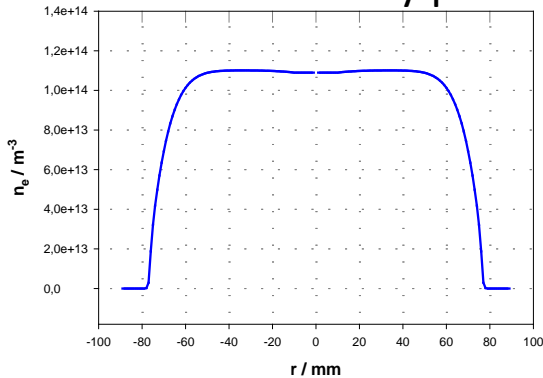
beam transport measurement



NNP diagnostics

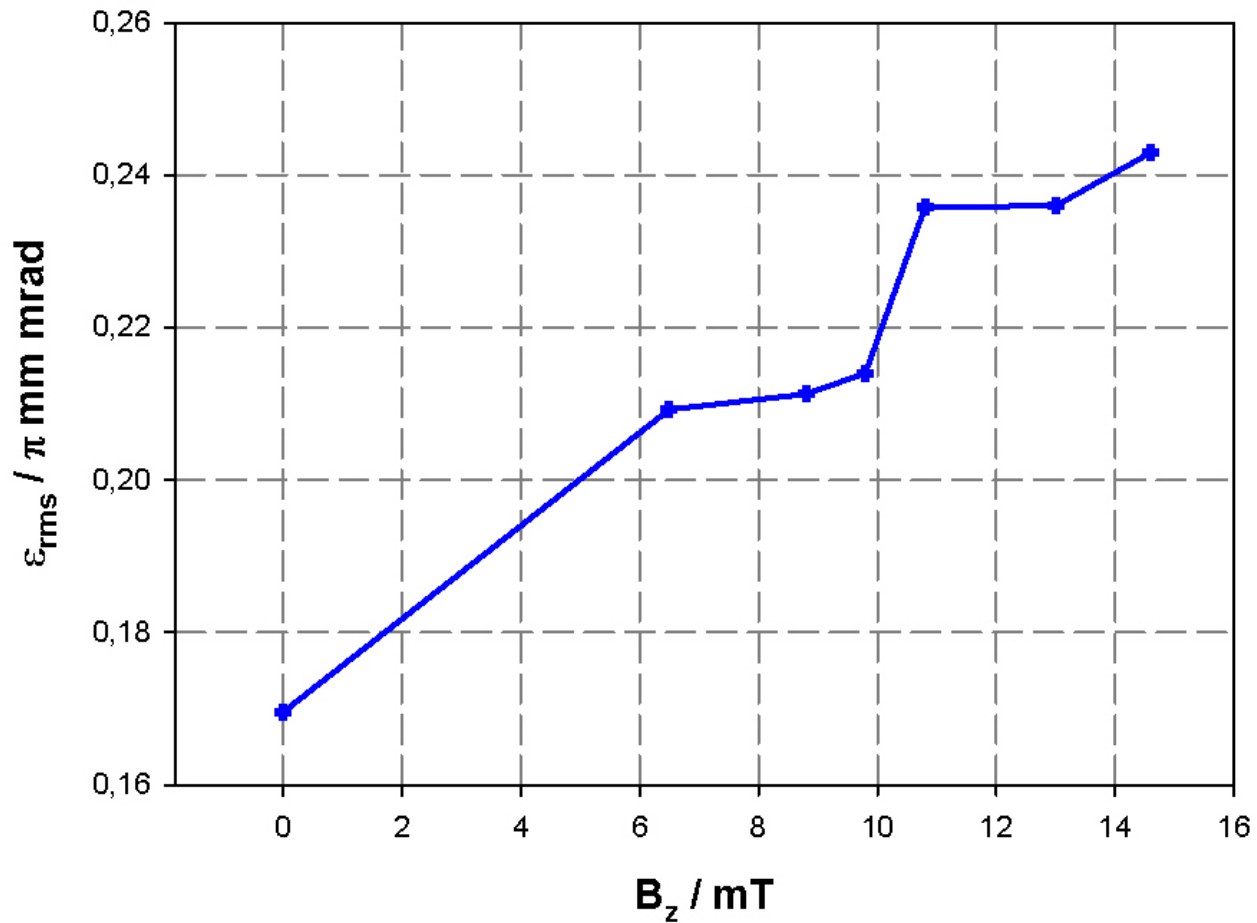
**NNP fluctuated,  
measurement not possible**

calculated density profile



## 3.4. High Current Measurements

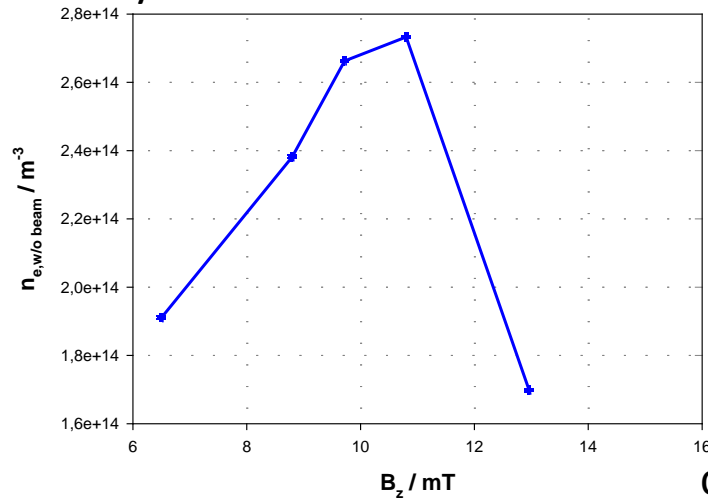
measured rms-emittance



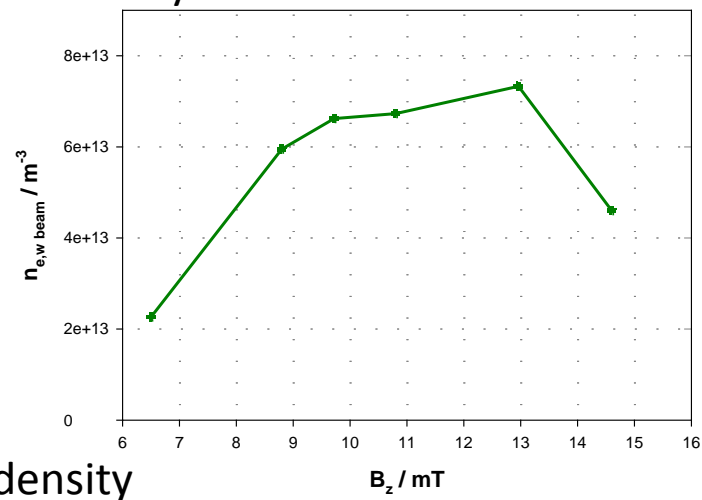


# 3.4. High Current Measurements

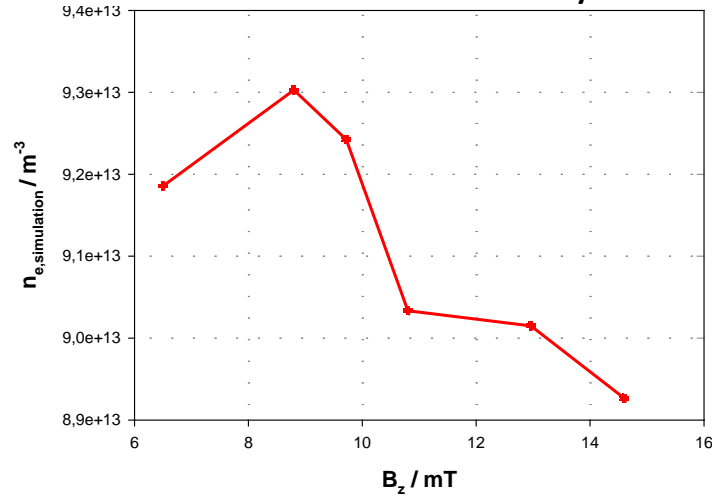
density measurement "without" beam



density measurement "with" beam



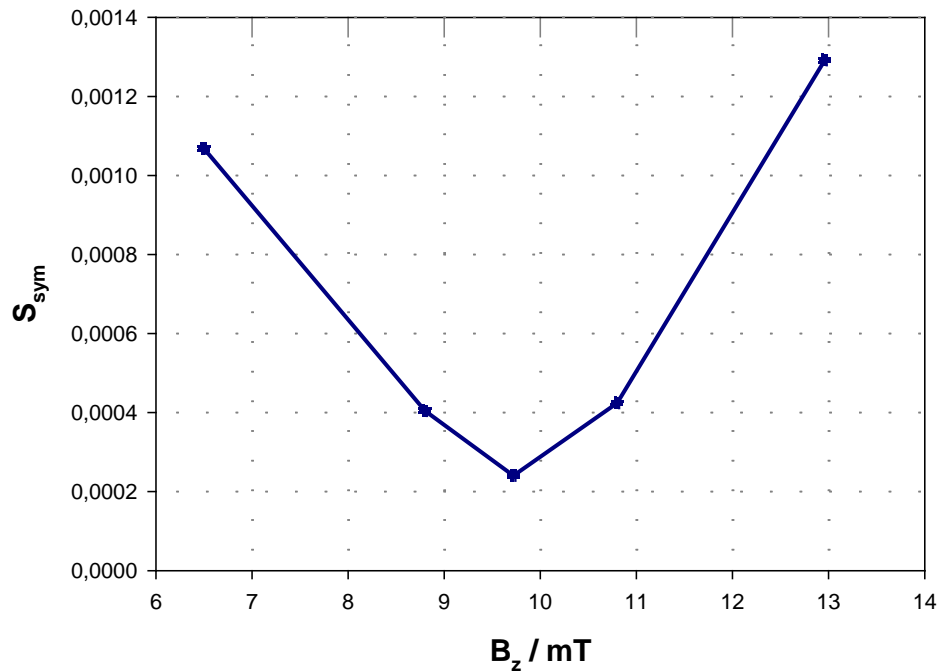
calculated density



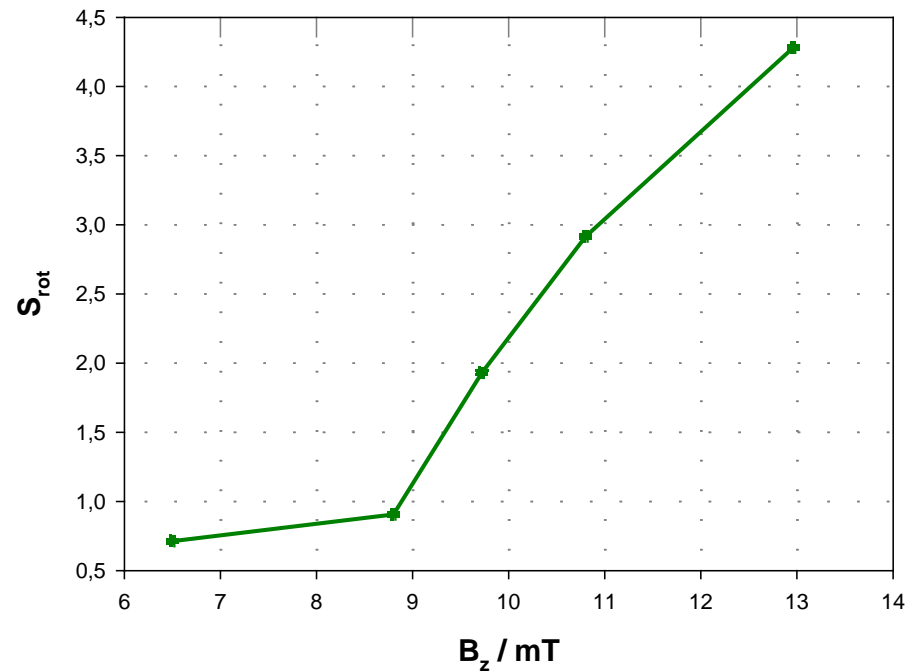
strong discrepancy between measurement and simulation

# 3.4. High Current Measurements

symmetry



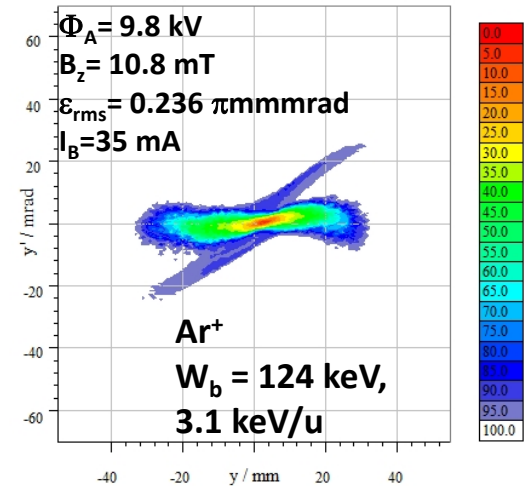
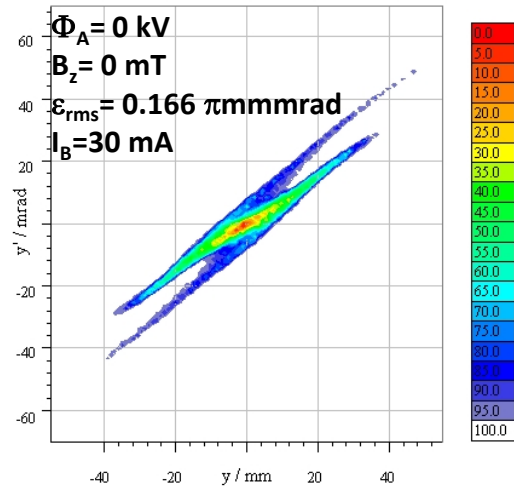
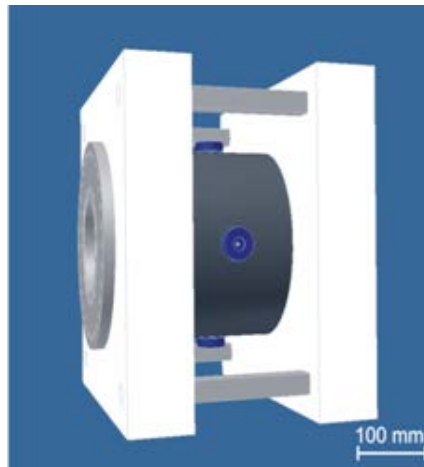
rotational symmetry



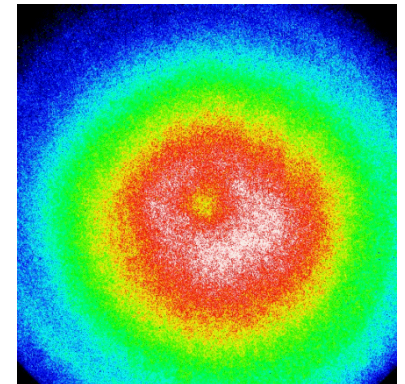
## 4. Summary

## 4.1. Summary

- Design and performance studies of prototype lens for GSI



- Development and evaluation of non-interceptive diagnostic methods
  - electron density measurement
  - temperature measurement
  - electron density distribution - symmetry and dynamics



Thank you for your attention!